Room Temperature rf
High Gradients: Physics, rf design and Technology
When Maxwell's equations just aren't enough

Part III: Breakdown in rf structures and design for high accelerating gradient

W. Wuensch
Fifth International Linear Collider School

30 October 2010

Overview of high-gradient rf behavior

From breakdown theory to rf cavities

OK, we have a picture of the physics of breakdown.

Now we're going to look specifically at the issues of breakdown in an rf cavity – that's why we're here.

First we will address:

- What does a high-power rf test look like?
- What happens when an rf structure breaks down?

Then we will address how the cavity design can influence the structure performance.

Finally just a few words about the technology of high-gradient rf structures.

What does a high-power rf test look like? What happens when an rf structure breaks down?

The basic layout of an rf test

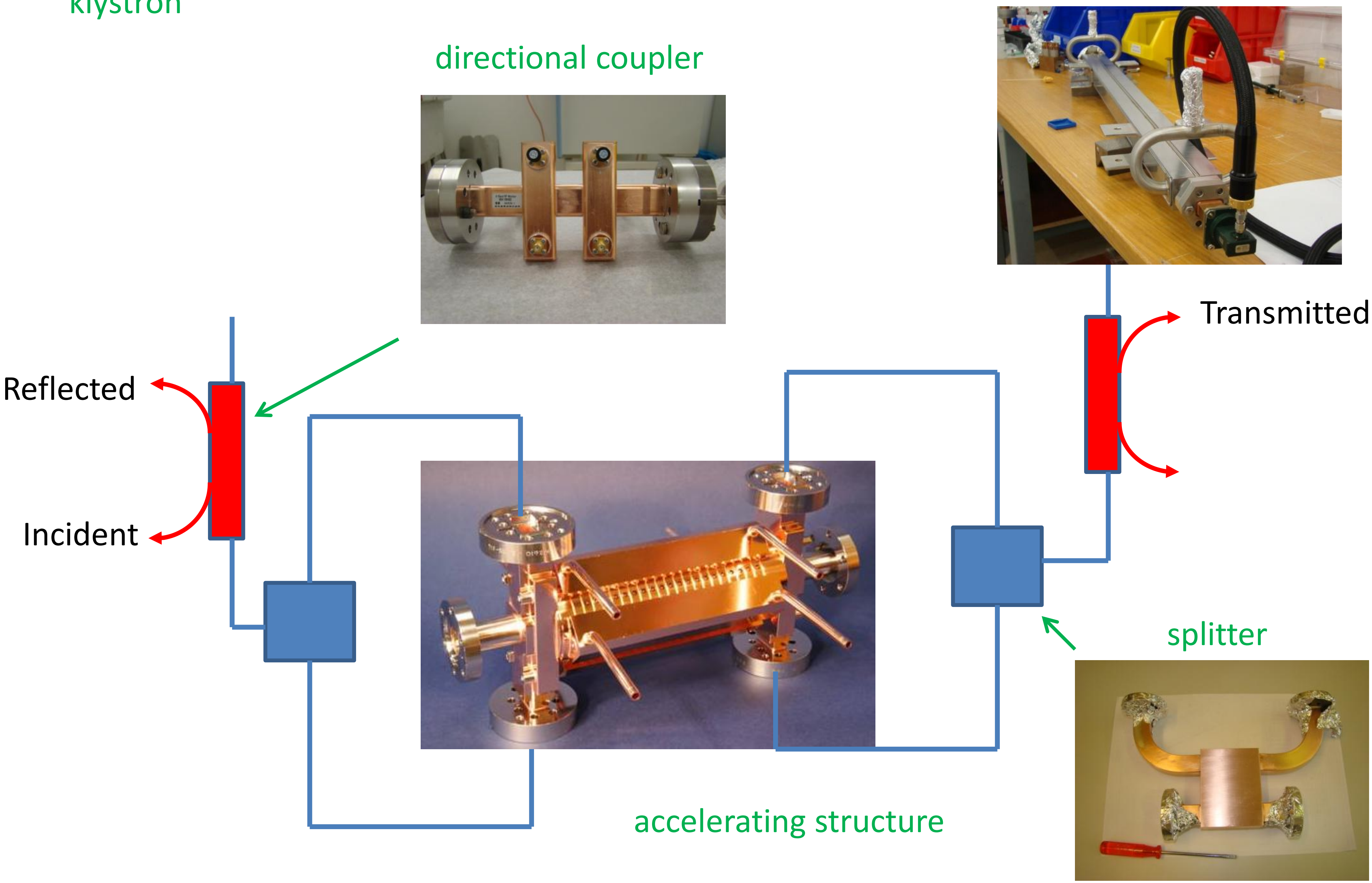

The basic layout of an rf test

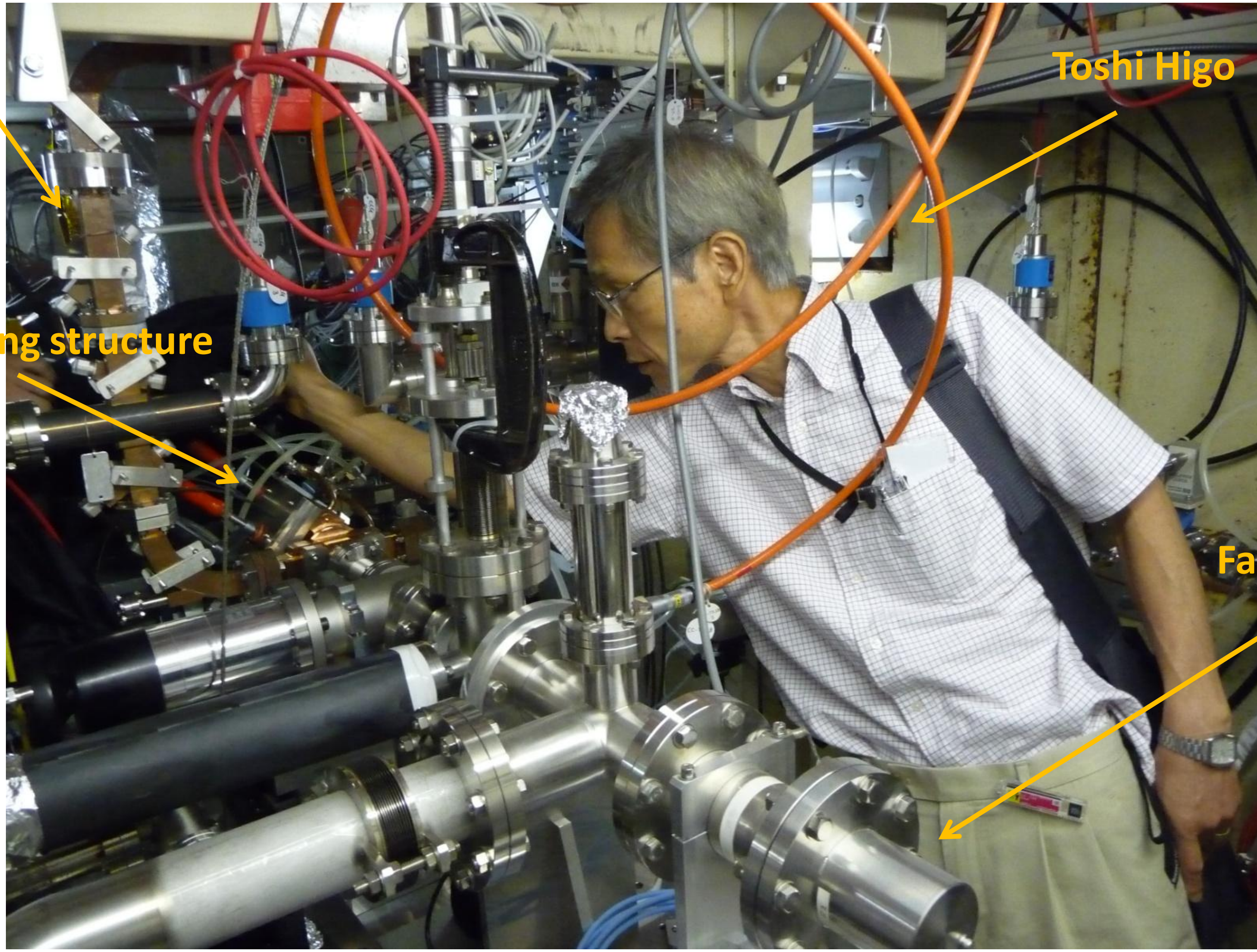

51+52 Normal pulse #36

Incident (F)

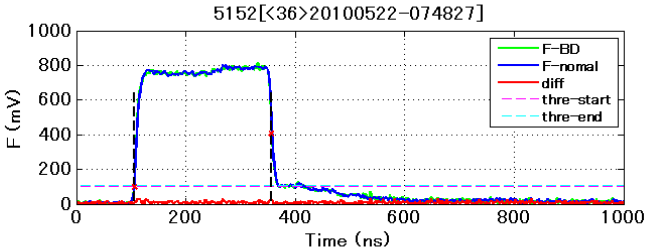

Reflected (Rs)

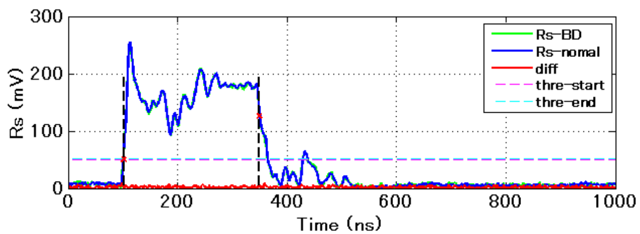

Transmitted (Tr)

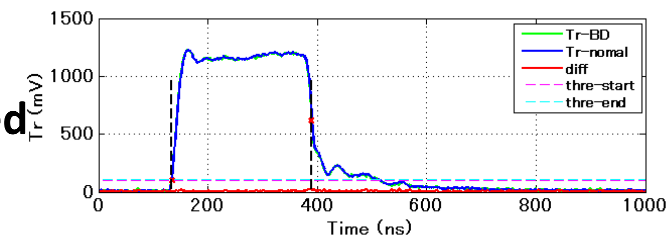

F RsX10 Tr

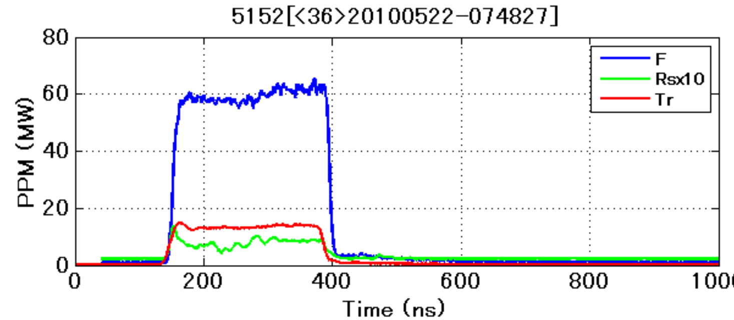

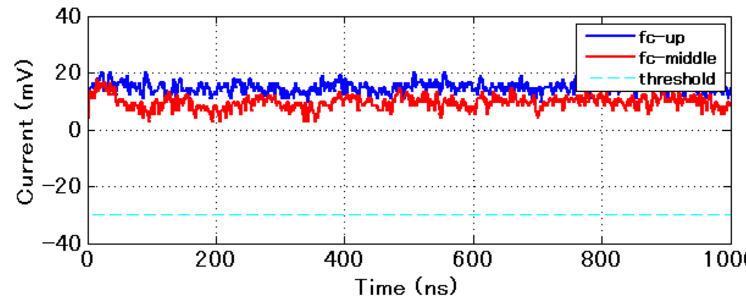

FC-UP FC-Mid Threshold

Last pulse

Last pulse but one

Difference between the two

Dashed lines = Analysis threshold

T. Higo, KEK
Test of TD18 structure

51+52 typical BD pulses
#72 Reflected RF back from klystron again

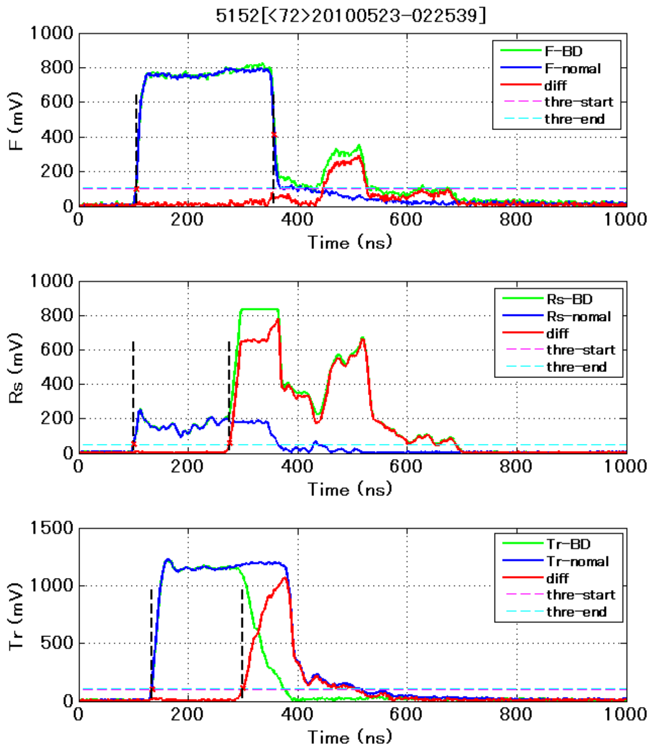

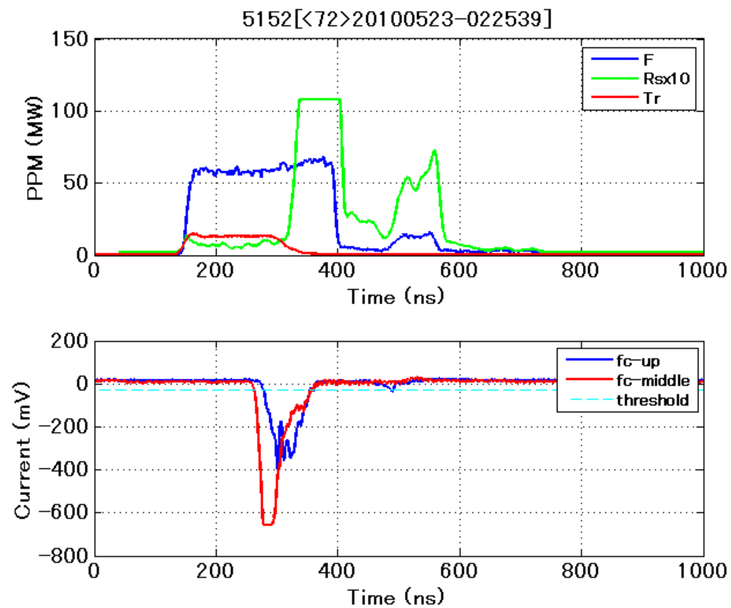

T. Higo, KEK
Test of TD18 structure

1: TW

Normal Waveforms of TD18
(s11 = -26.55 dB, s21 = -1.37 dB)

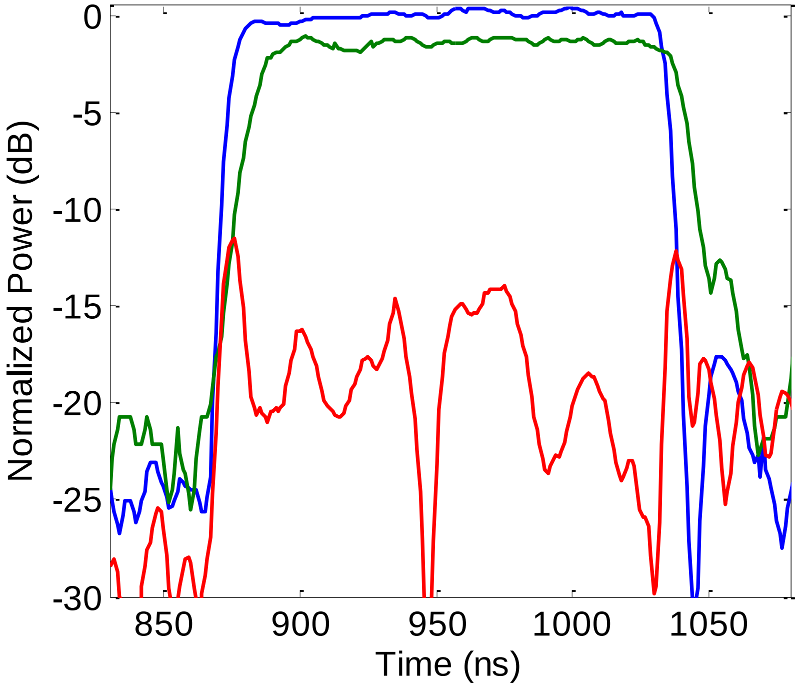

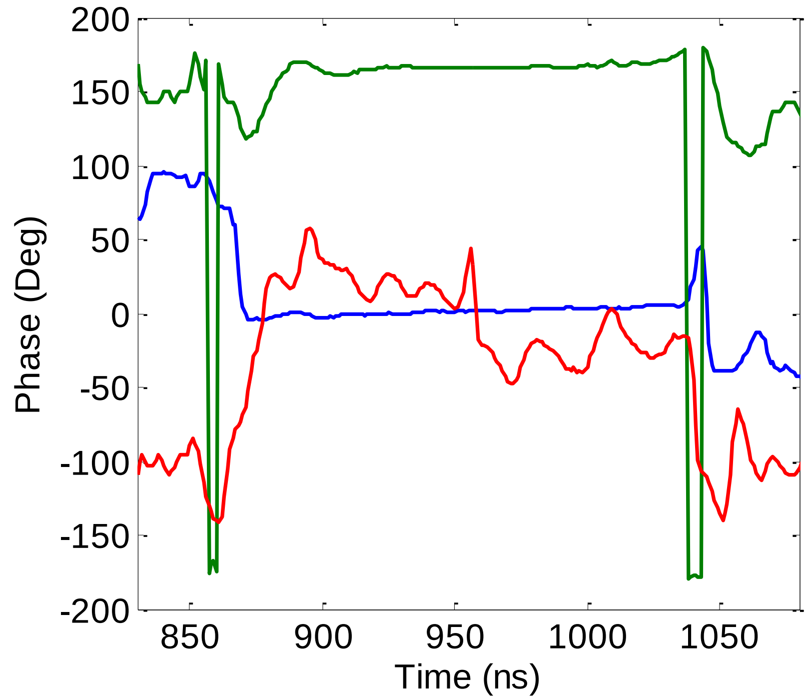

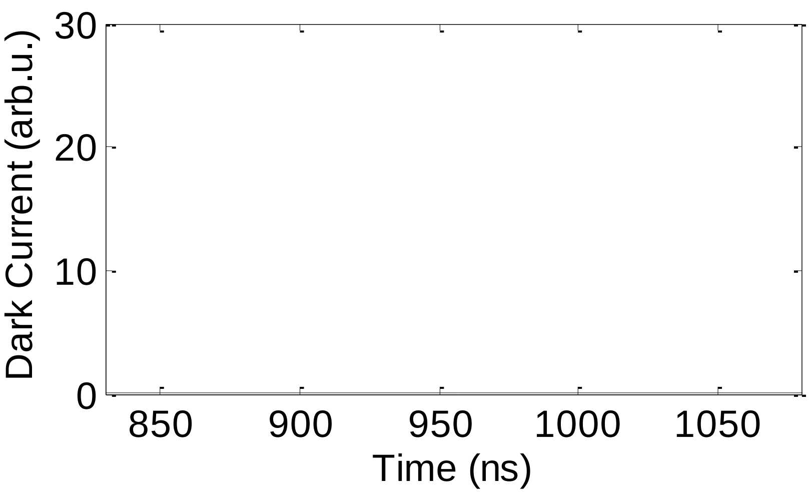

Blue – Input Forward, Green – Output Forward, Red – Input Reflected, Black – dark current.

F. Wang, SLAC
Test of TD18 structure

1: TW

Breakdown Waveforms of TD18

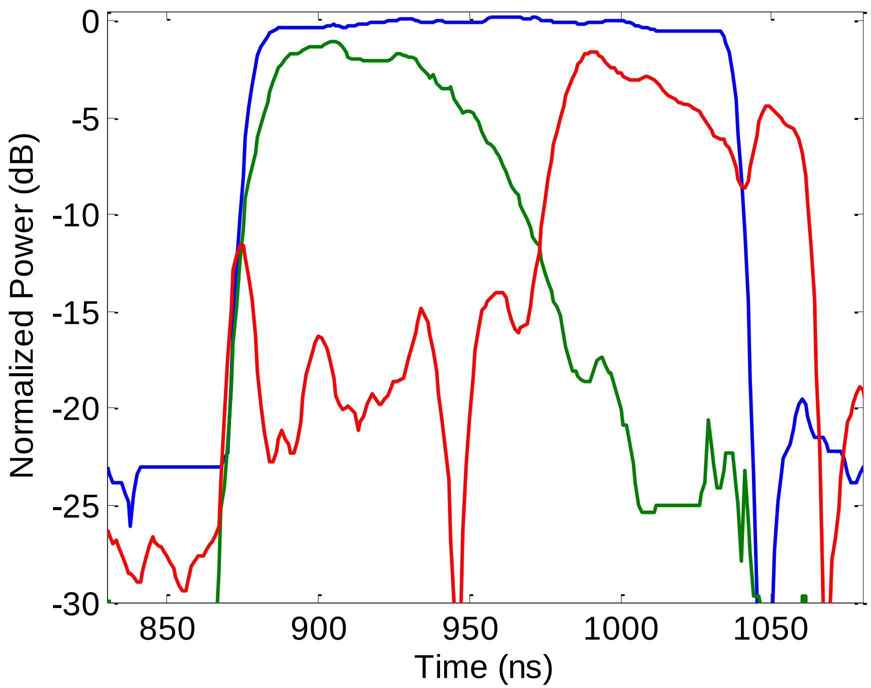

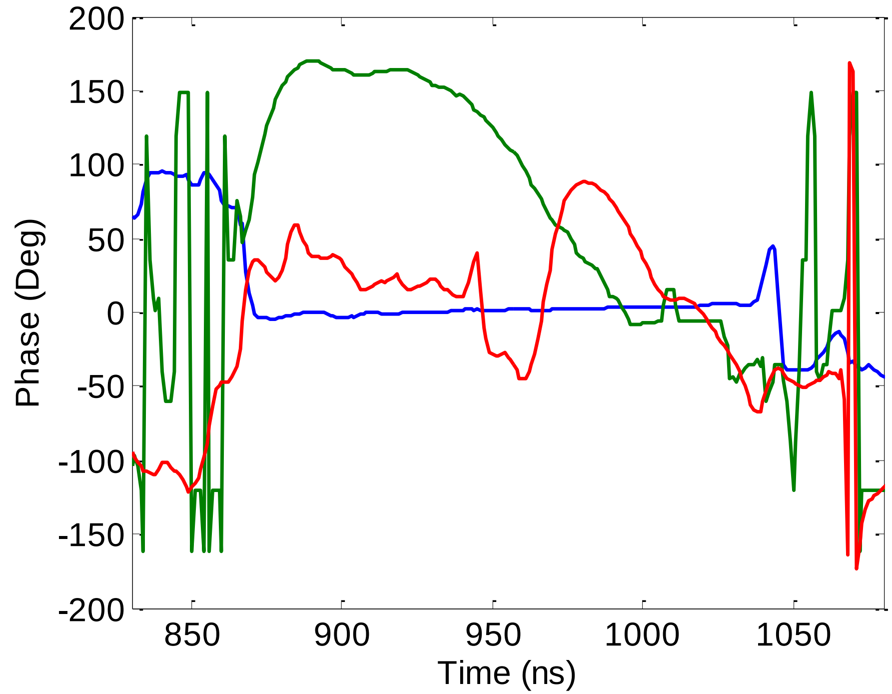

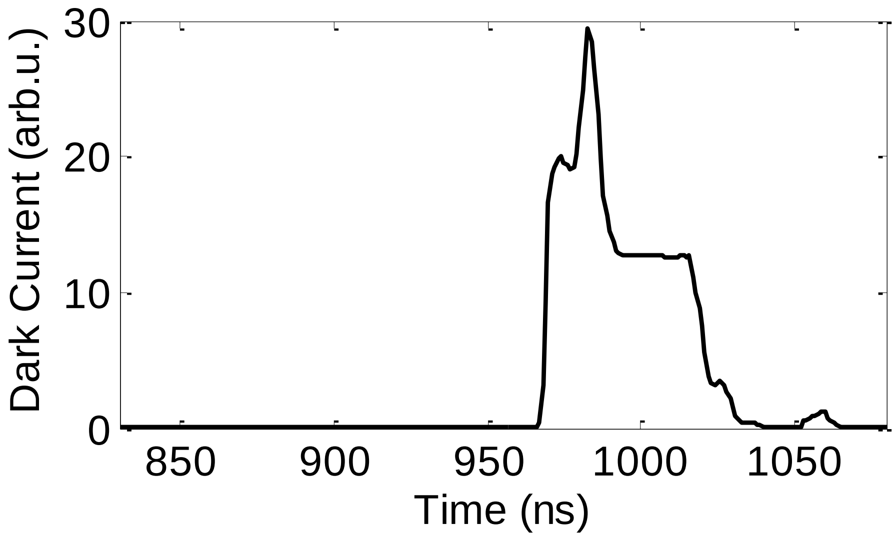

Blue – Input Forward, Green – Output Forward, Red – Input Reflected, Black – dark current.

F. Wang, SLAC
Test of TD18 structure

High Power Operation History

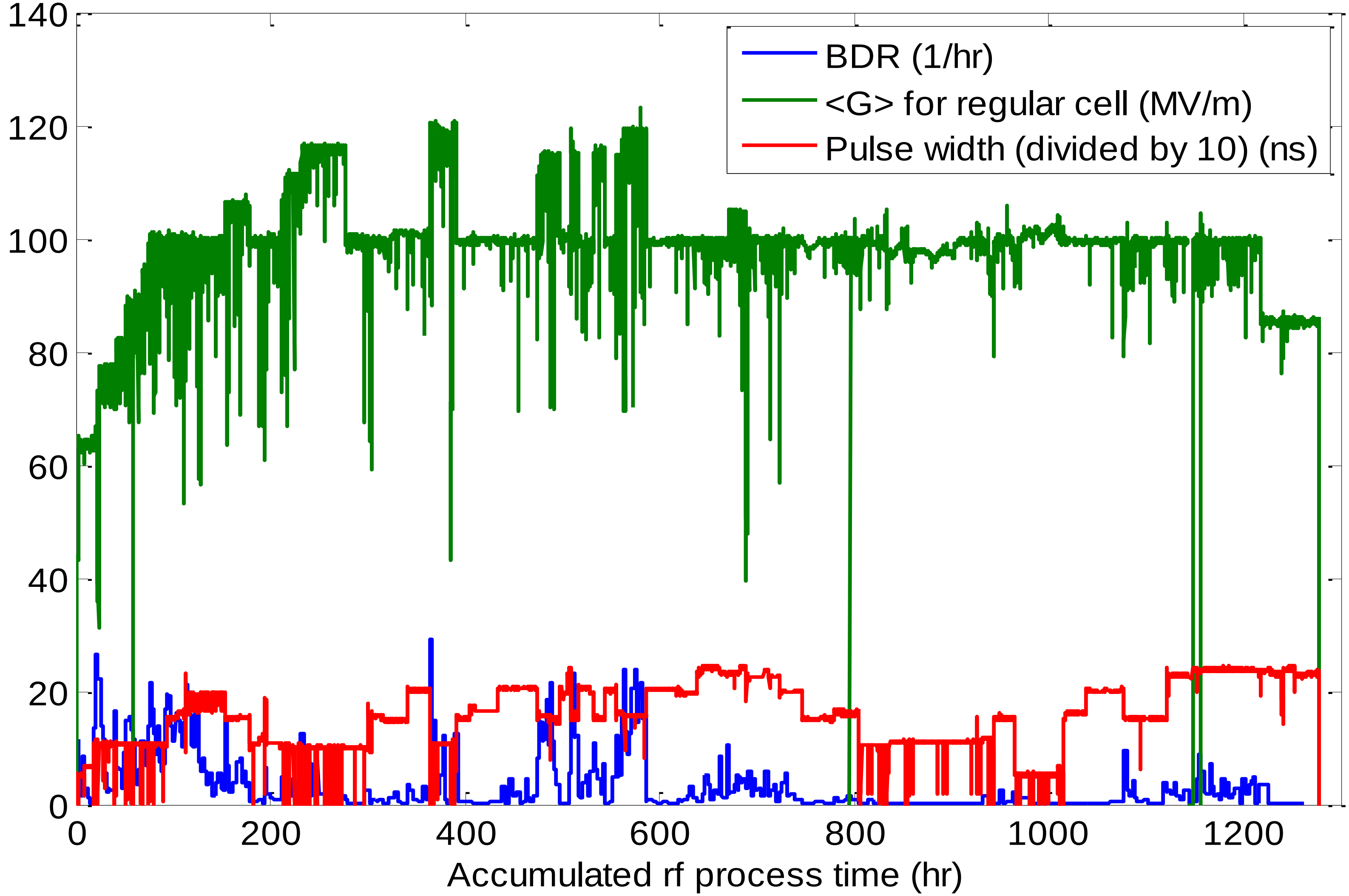

Final Run at 230 ns: 94 hrs at 100 MV/m w BDR = 7.6e-5
60 hrs at 85 MV/m w BDR = 2.4e-6

F. Wang, SLAC

Conditioning history

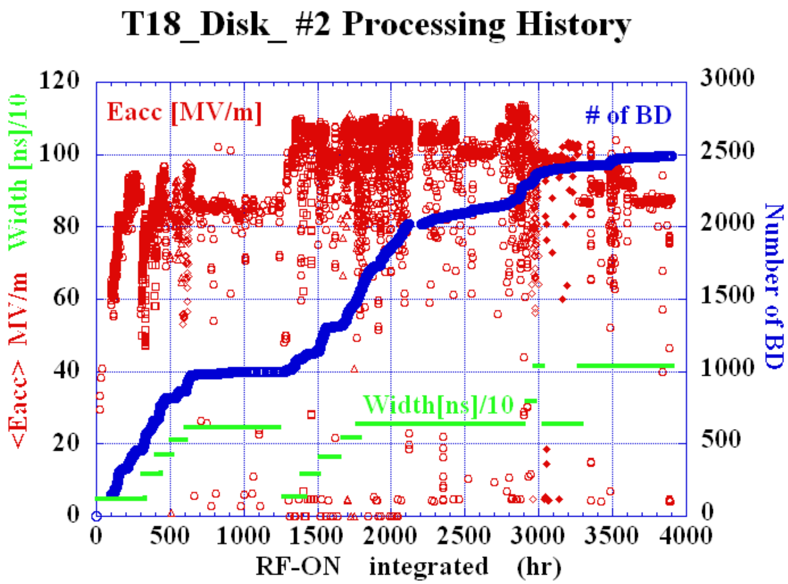

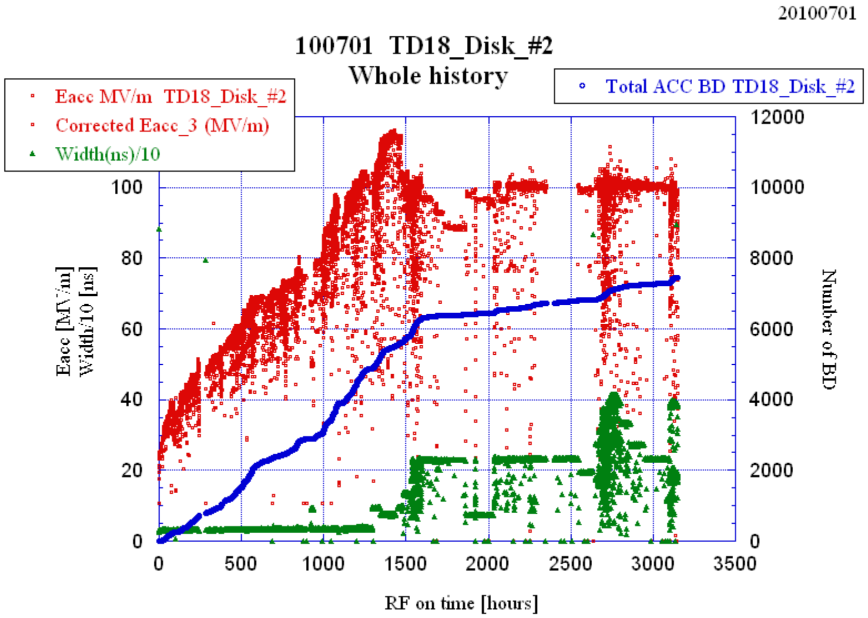

TD18_Disk_#2 BDR evolution

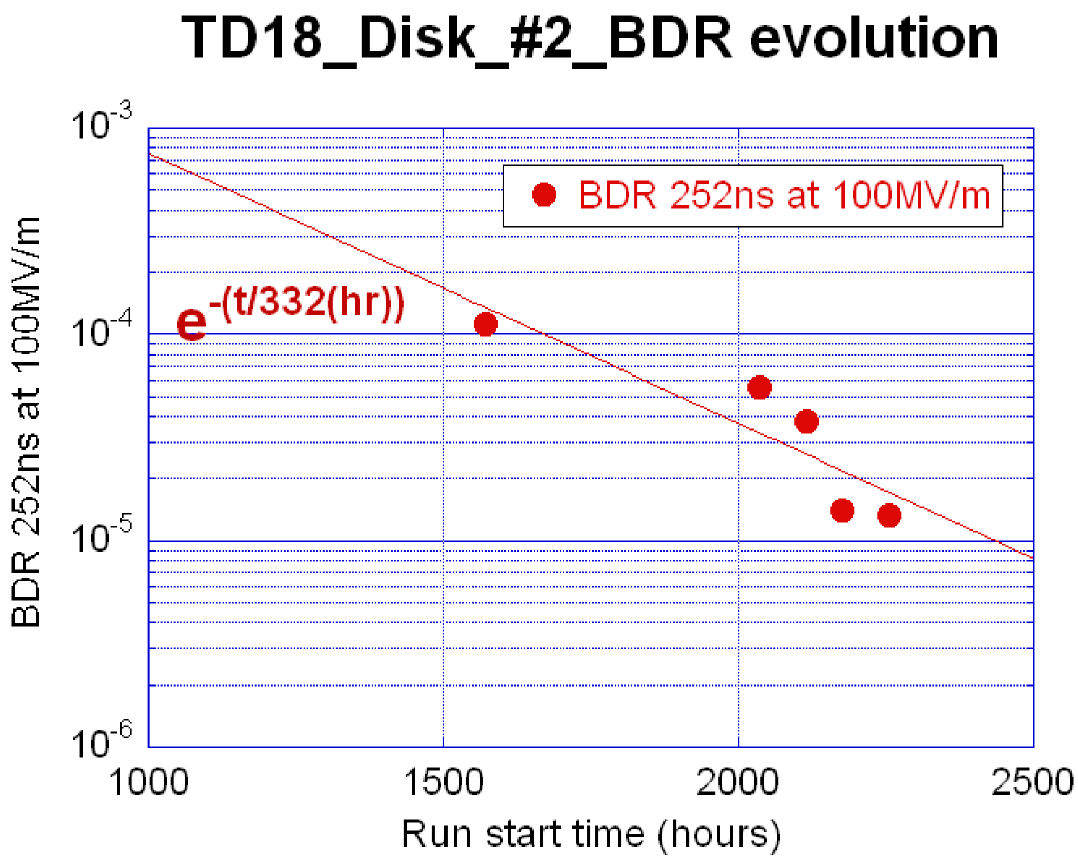

The most important dependencies: gradient, pulse length, geometry, running time (and frequency but not today)

CERN/KEK/SLAC T18 structure tests

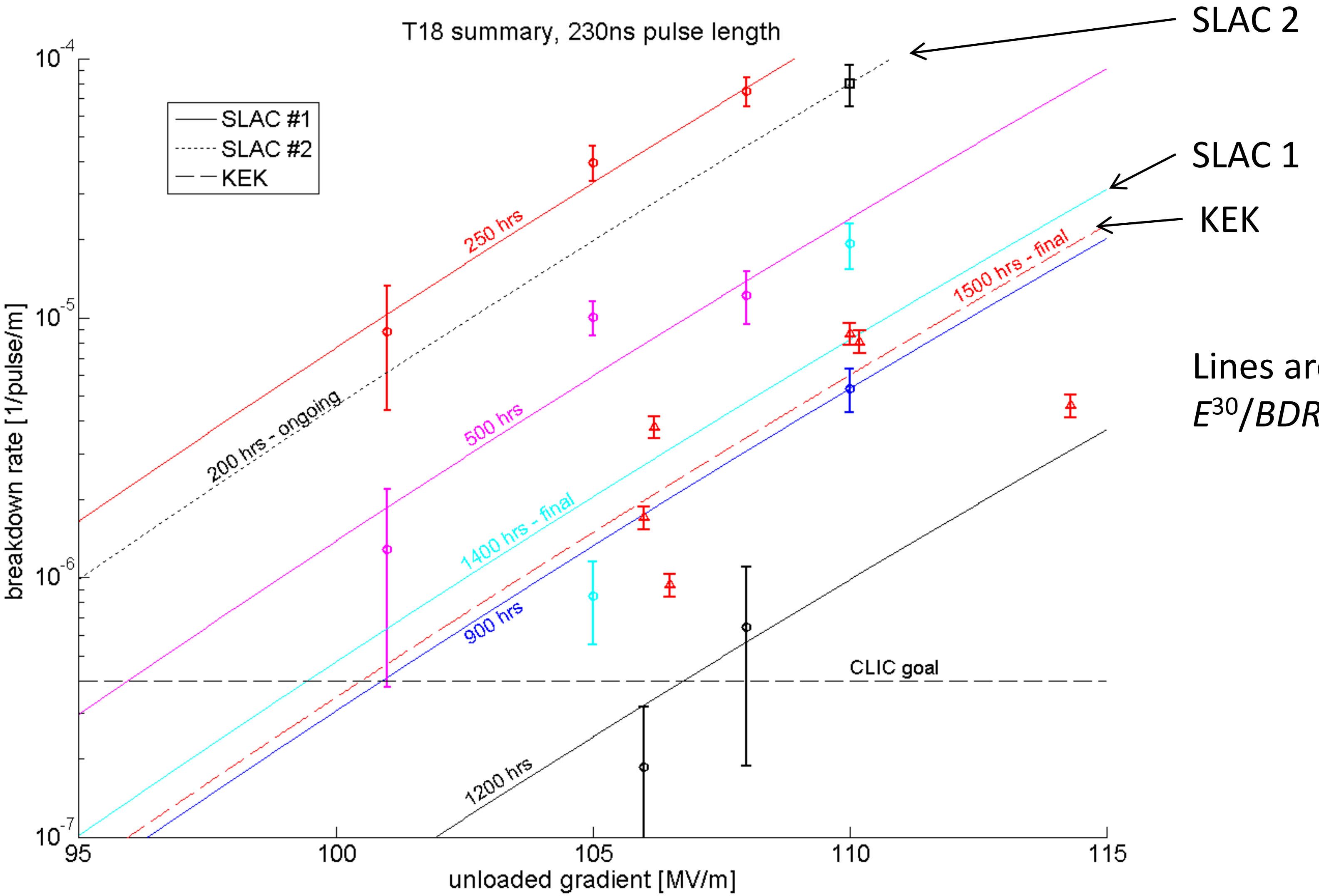

Lines are
E^{30}/BDR=const

BDR versus Gradient scaling

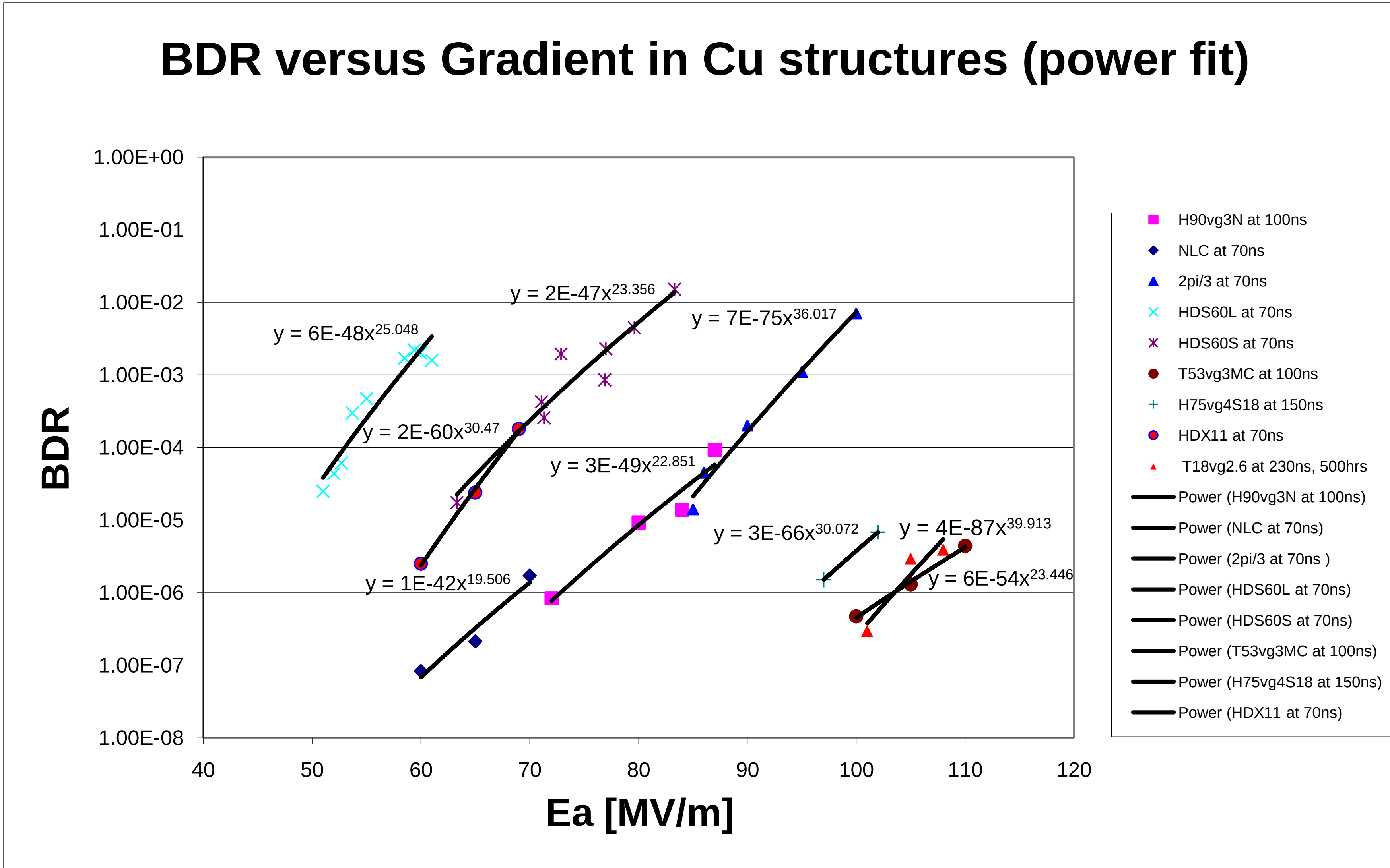

Power fit can be done with the same power for all gradients

BDR versus Gradient scaling

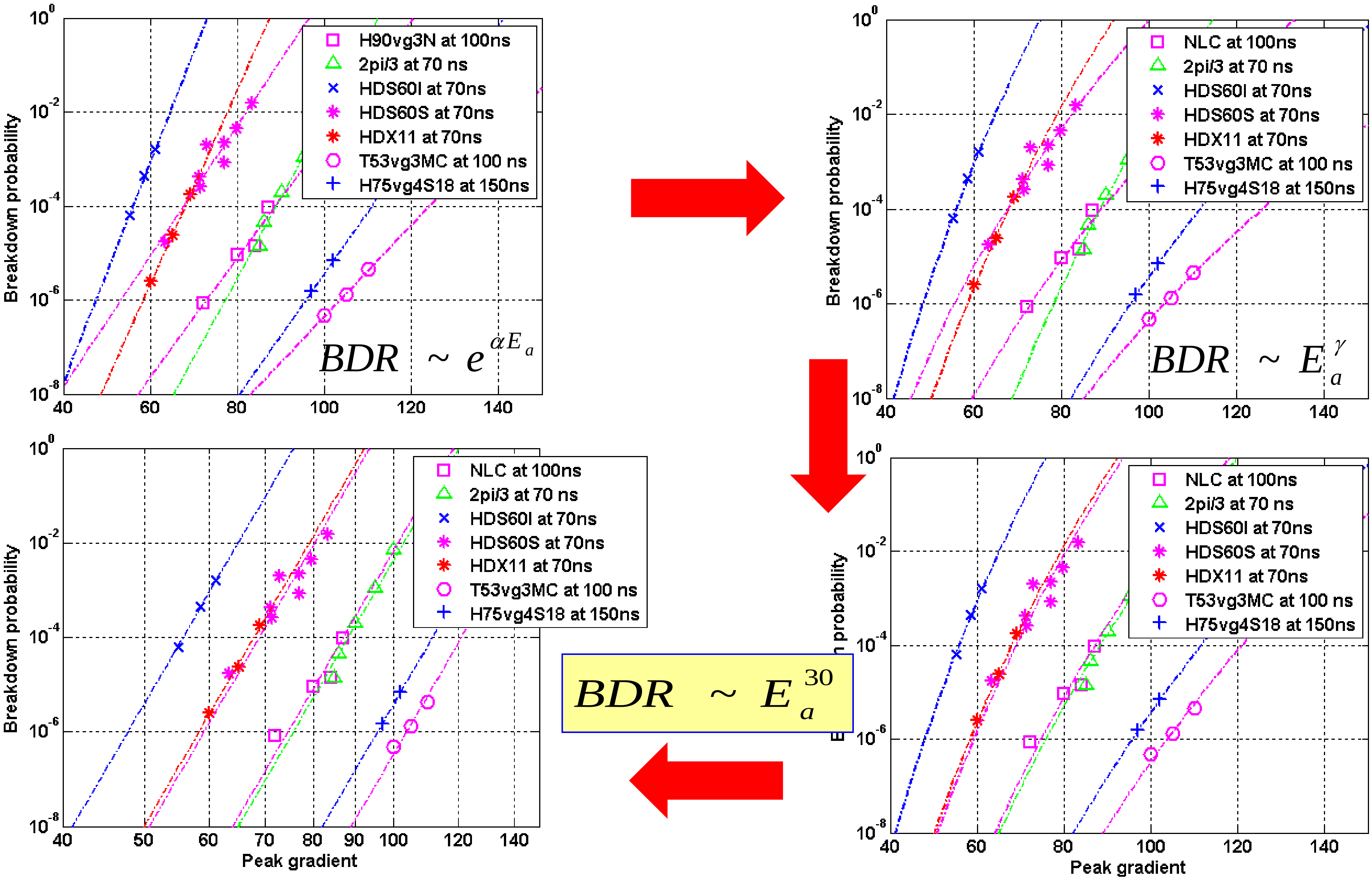

$$BDR \sim E_a^{30}$$

Gradient versus pulse length scaling

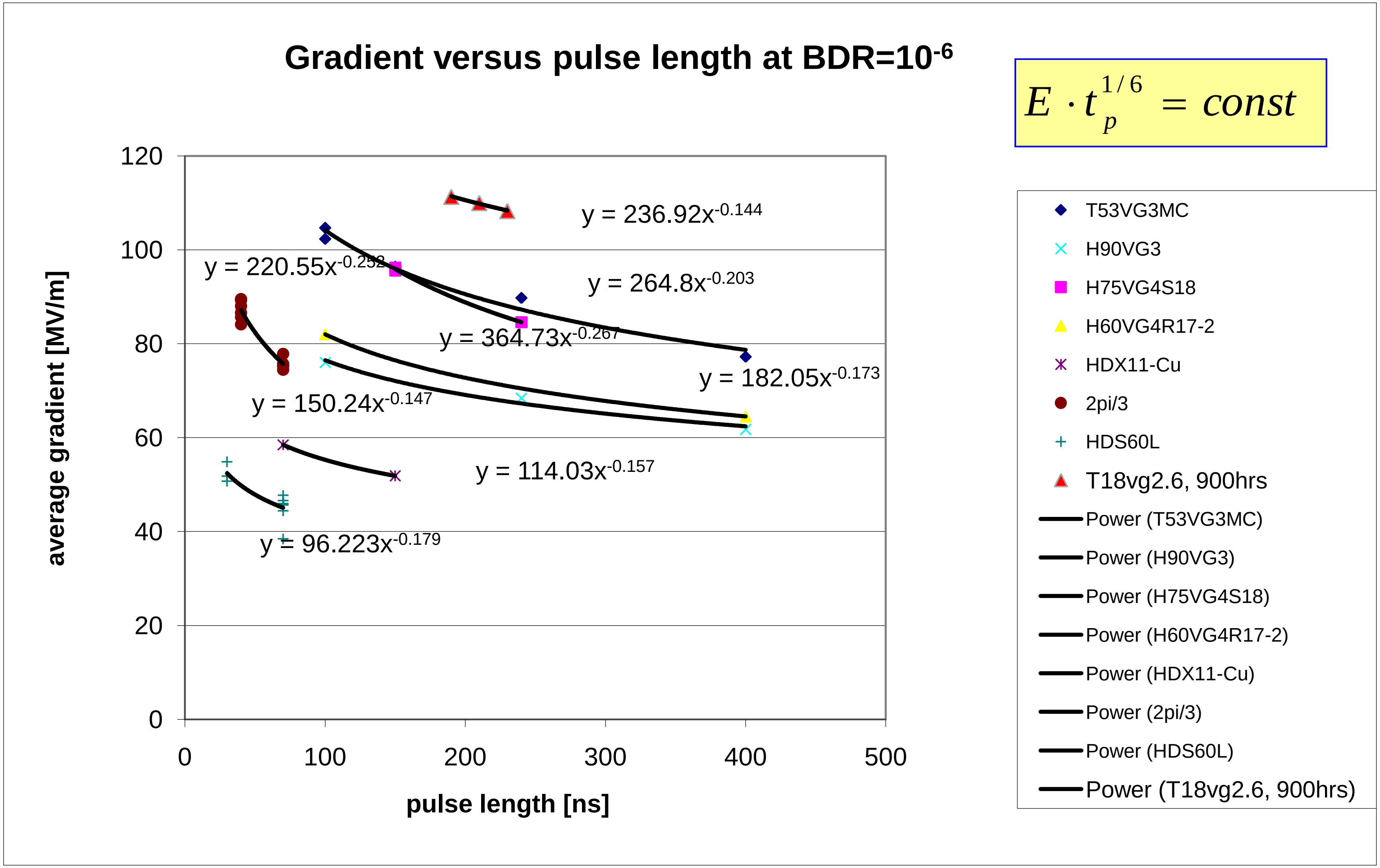

$$E \cdot t_p^{1/6} = const$$

N.B. This is very well known scaling law being confirmed again and again

Gradient and pulse length dependencies in KEK tests

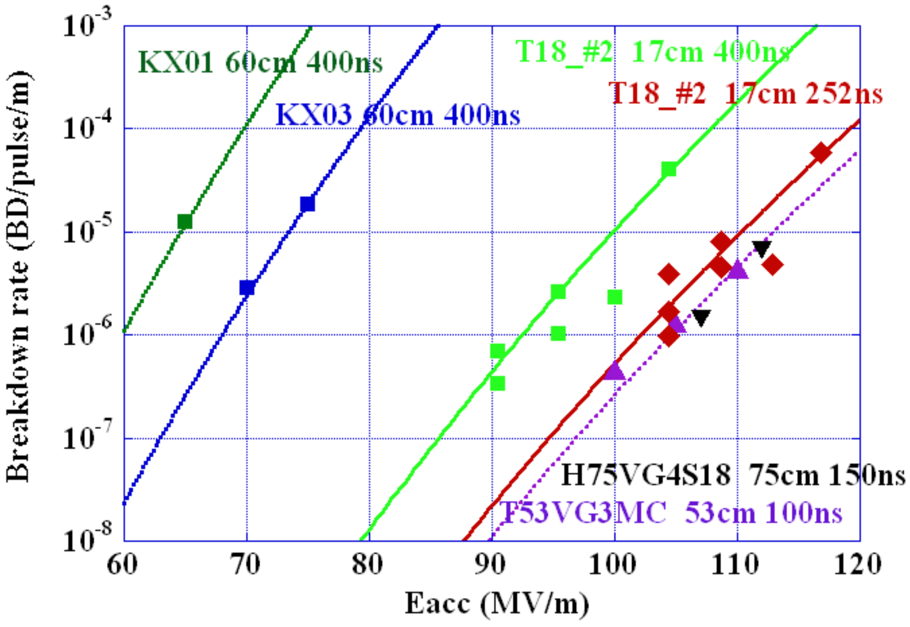

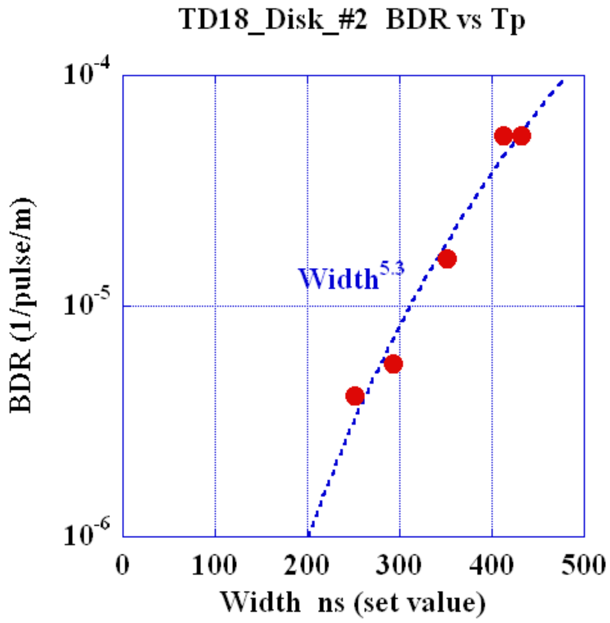

Breakdown rate data from single cell standing-wave cavity tests at SLAC

1C-SW-A2.75-T2.0-Cu-SLAC-#1

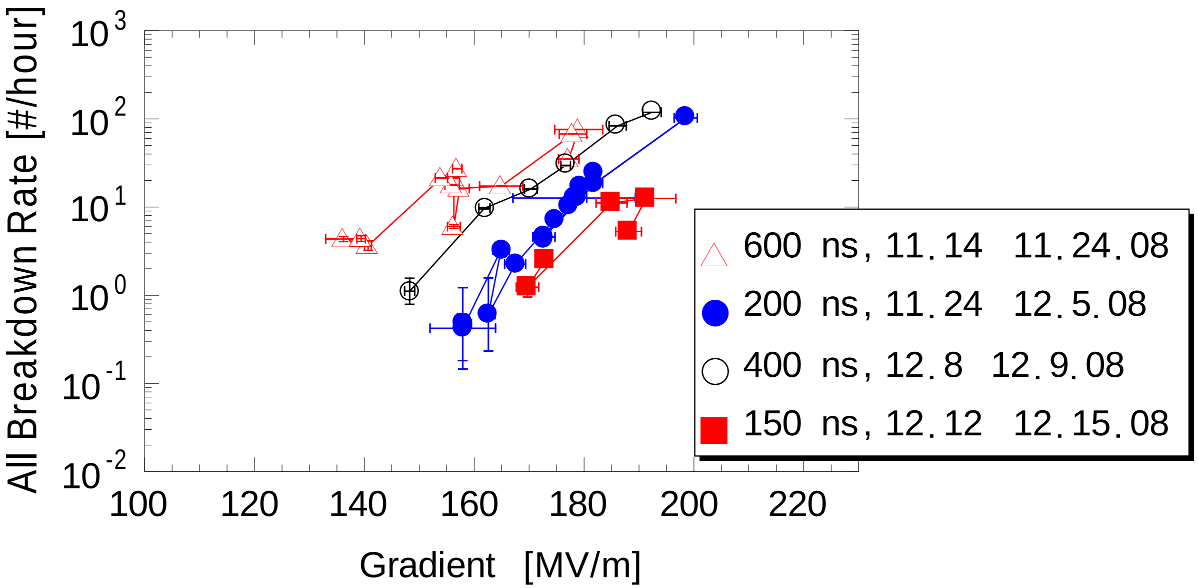

V. Dolgashev, SLAC

Summary on gradient scaling

For a fixed pulse length

$$BDR \sim E_a^{30}$$

For a fixed BDR

$$E_a \cdot t_p^{1/6} = const$$

$$\frac{E_a^{30} \cdot t_p^5}{BDR} = const$$

- In **a** Cu structure, ultimate gradient E_a can be scaled to certain BDR and pulse length using above power law. It has been used in the following analysis of the data.
- The aim of this analysis is to find a field quantity X which is geometry independent and can be scaled among **all** Cu structures.

Quantifying geometrical dependence of high-power performance

Importance of geometric dependence - motivation

As you have seen in Daniel's, Erk's and Alexej's presentations, there is a strong interplay between the rf design of accelerating structures and the overall performance of the collider.

One of the strongest dependencies is emittance growth as function of the average iris aperture which acts through transverse wakefields.

The iris aperture also influences required peak power and efficiency through its effect on group velocity.

But crucially the iris aperture has an extremely strong influence on achievable accelerating gradient.

Very generally, we expect that the gradient of an rf structure should be calculable from its geometry if material and preparation are specified.

The big questions

Where does such a geometrical dependency come from?

Can we quantify the dependence of achievable accelerating gradient on the geometry?

Trying to understand, derive and quantify geometrical dependence has been a significant effort because an essential element of the overall design and optimization of the collider.

The basic approach

The basic element is to express our high-power limits as a function of the unperturbed fields inside our structures – like the electric field limit in dc spark.

So first we are going to make sure that we have a feel for how those fields vary as a function of geometry.

We use a specific example of iris variation for a fixed phase advance in a travelling wave structure.

Field distribution

Electric field (V/m)

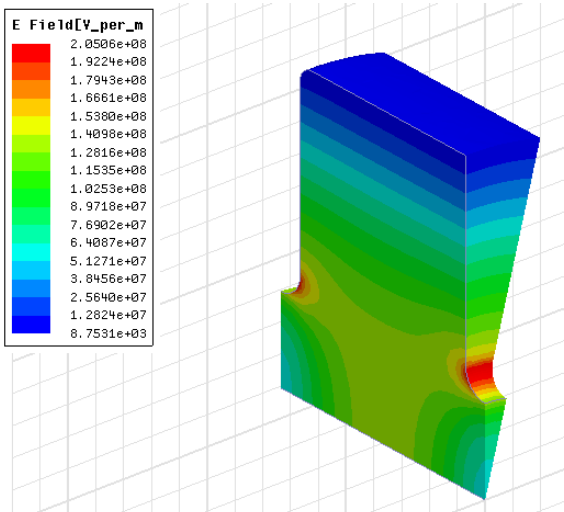

Magnetic field (A/m)

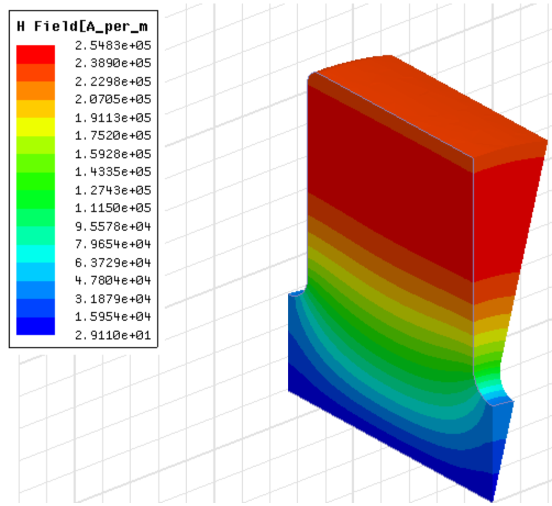

Poynting vector (W/m^2)

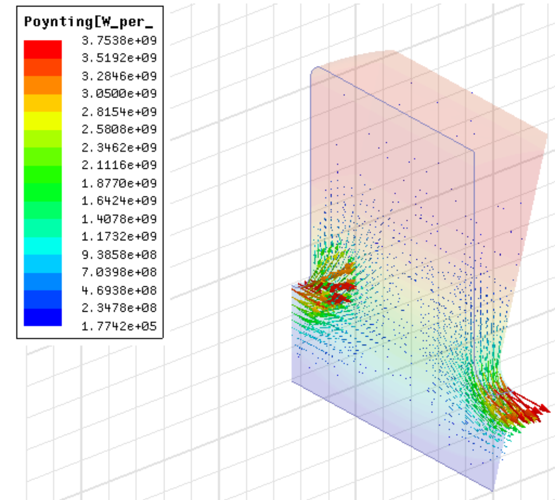

- Simulation in HFSS12
- Field values are normalized to accelerating gradient, E_{acc}=100MV/m
- Frequency: 11.424GHz
- Phase advance per cell: 120 degree
- *Iris radius*: 3mm
- v_g /*c*= 1.35%

Parameters v.s. iris

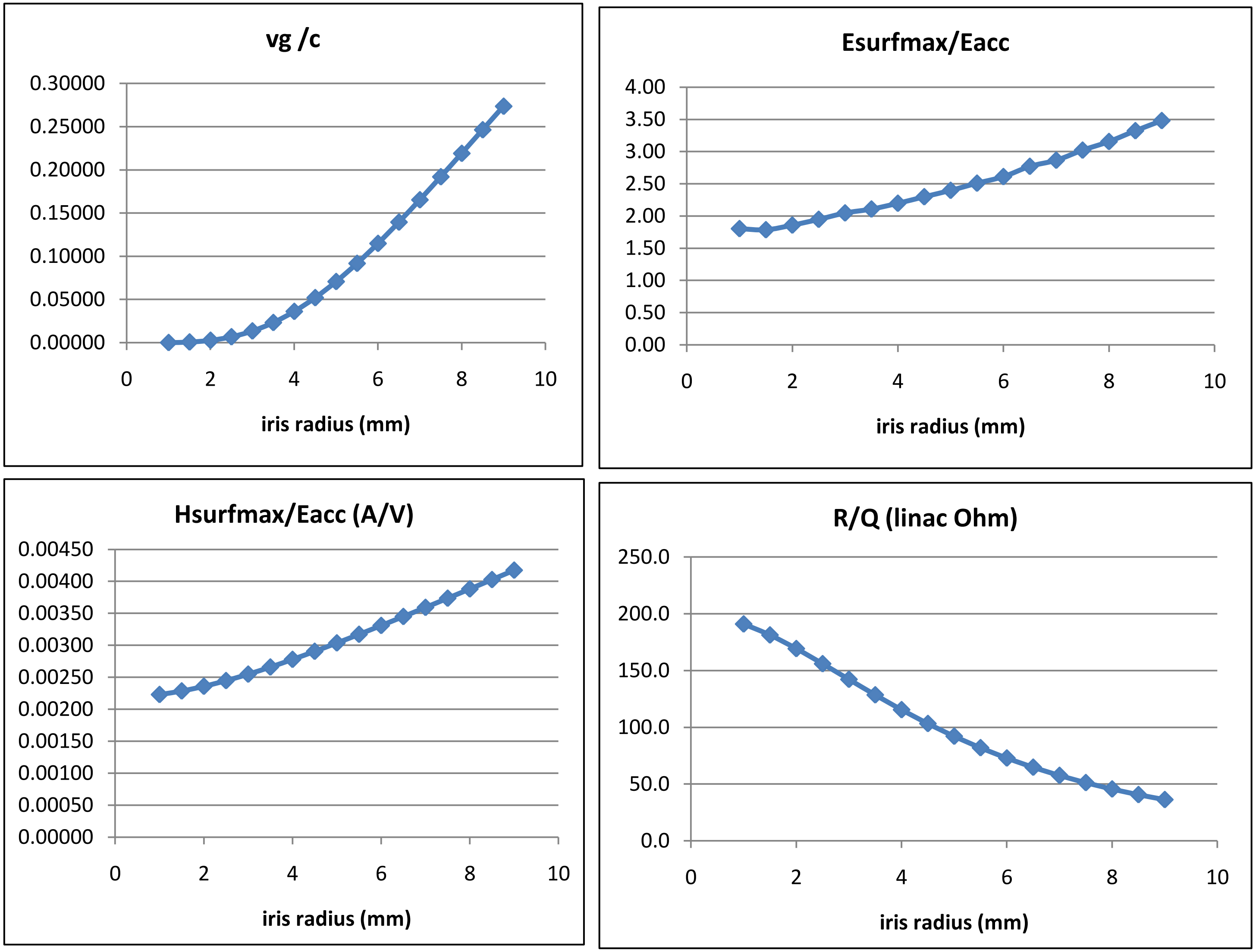

Simulation in HFSS12
Iris thickness: 1.66mm
Frequency: 11.424GHz
Phase _adv/cell: 120 degree

$$R/Q = V^2_{acc}/(\omega U)$$

Overview of how different types of structures behave – from accelerating structures to PETS

Achieving high gradients has been a high profile concern for CLIC and NLC/JLC since roughly 2000. Here are the target specifications we have had:

	frequency [GHz]	Average loaded gradient [MV/m]	Input (output for PETS) power [MW]	Full pulse length [ns]
NLC/JLC	11.424	50	55	400
CLIC pre-2007				
Accelerating	29.928	150	150	70
PETS	29.985	-5.7	642	70
CLIC post 2007				
Accelerating	11.994	100	64	240
PETS	11.994	-6.3	136	240

Trying to achieve these specifications has resulted in the test of many structures of diverse rf design over the years.

The preparation and testing conditions of the test structures which were built were not always the same – these processes also evolved over the period the structures were being developed.

But the wide variety of structure geometries were tested under reasonably similar conditions.

So we have used this unique set of data to try to understand and then quantify the geometrical dependency of gradient.

List of structures from CLIC and NLC/JLC testing programs

number	RF design name	f [GHz]	dphi [deg]	a1 [mm]	vg1 [%]
1	DDS1	11.424	120	5.7	11.7
2	T53VG5R	11.424	120	4.45	5
3	T53VG3MC	11.424	120	3.9	3.3
4	H90VG3	11.424	150	5.3	3
5	H60VG3	11.424	150	5.3	2.8
6	H60VG3R18	11.424	150	5.5	3.3
7	H60VG3R17	11.424	150	5.3	3.6
8	H75VG4R18	11.424	150	5.3	4
9	H60VG4R17	11.424	150	5.68	4.5
10	HDX11-Cu	11.424	60	4.21	5.1
11	CLIC-X-band	11.424	120	3	1.1
12	T18VG2.6-In	11.424	120	4.06	2.6
13	T18VG2.6-Out	11.424	120	2.66	1.03
14	T18VG2.6-Rev	11.424	120	2.66	1.03
15	T26VG3-In	11.424	120	3.9	3.3
16	T26VG3-Out	11.424	120	3.2	1.65
17	TD18_KEK_In	11.424	120	4.06	2.4
18	TD18_KEK_Out	11.424	120	2.66	0.9
19	SW20A3p75	11.424	180	3.75	0
20	SW1A5p65T4p6	11.424	180	5.65	0
21	SW1A3p75T2p6	11.424	180	3.75	0
22	SW1A3p75T1p66	11.424	180	3.75	0
23	2pi/3	29.985	120	1.75	4.7
24	pi/2	29.985	90	2	7.4
25	HDS60-In	29.985	60	1.9	8
26	HDS60-Out	29.985	60	1.6	5.1
27	HDS60-Rev	29.985	60	1.6	5.1
28	HDS4Th	29.985	150	1.75	2.6
29	HDS4Th	29.985	150	1.75	2.6
30	PETS9mm	29.985	120	4.5	39.8

All high-power test data will be normalized to:
200 ns pulse length
and
$1x10^{-6}$ 1/pulse breakdown rate

Standing wave (structures 19–22)

30 GHz (structures 23–30)

Quantitative comparison of selected parameters

Objective first – accelerating gradient

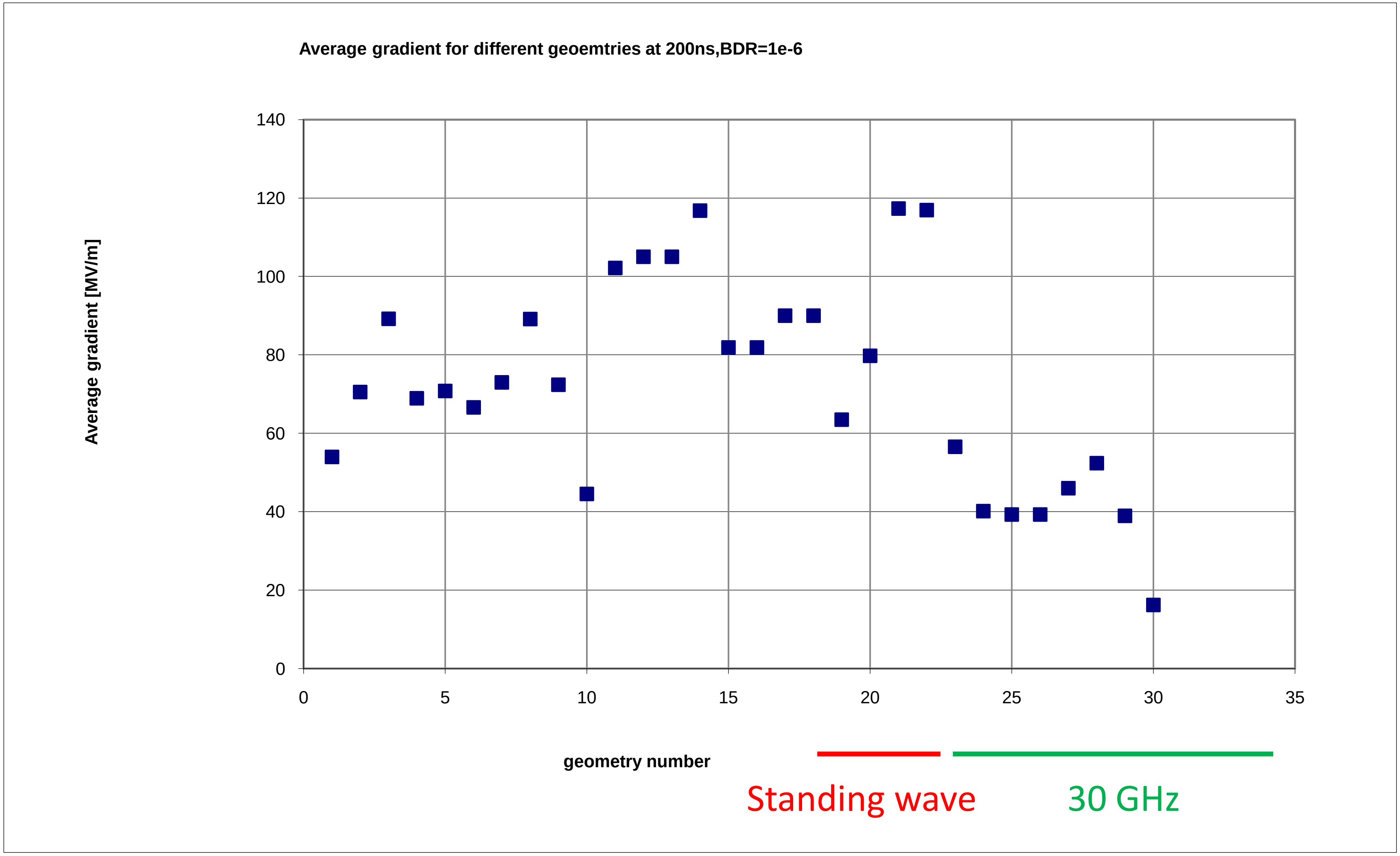

Most obvious – surface electric field

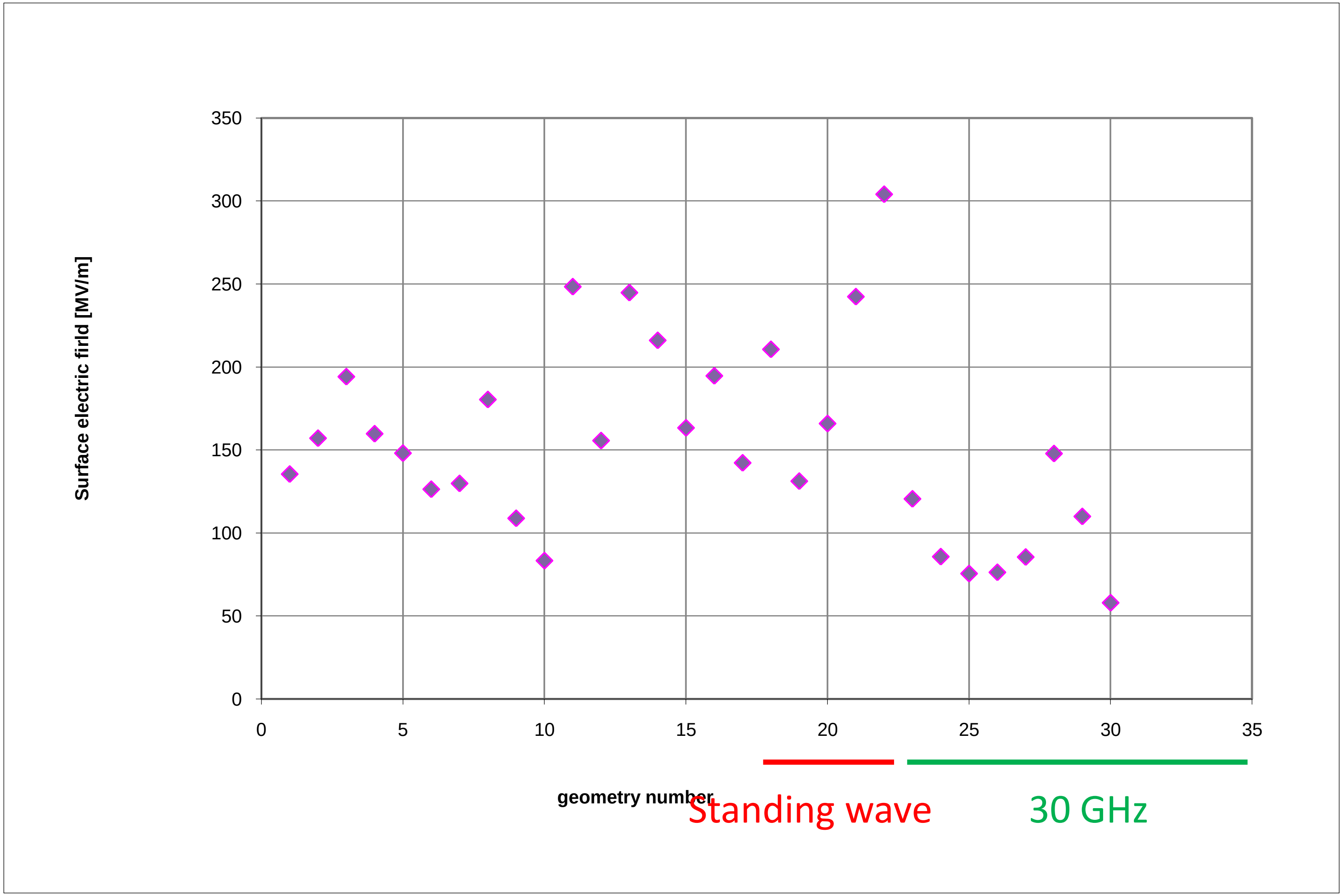

How about power flow?

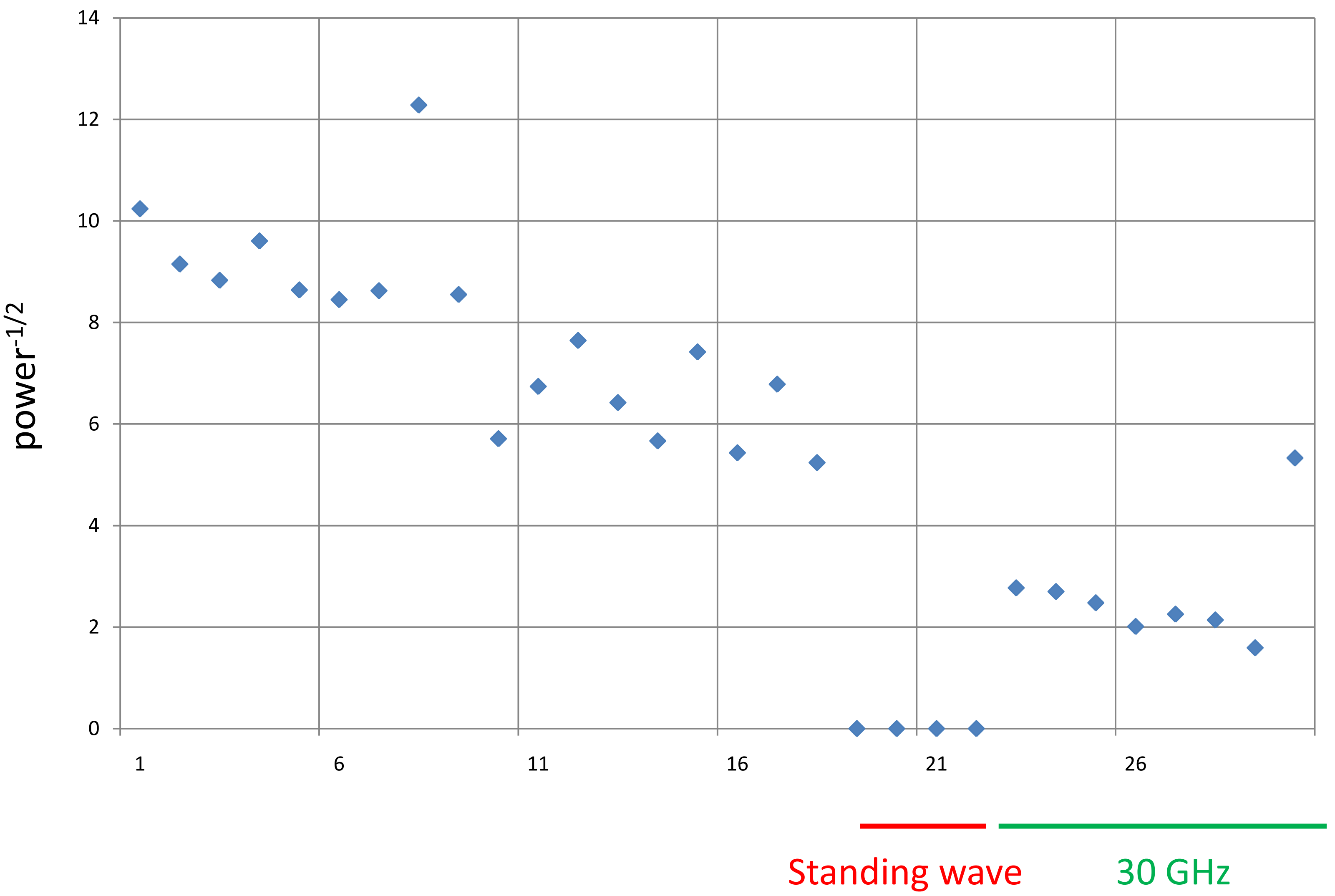

High-power scaling laws: P/C and S_c

Let's consider the very simple idea that larger structures can carry more power.

A couple of physical arguments to justify a limit based on power "density" are,

1. A certain level of power is needed to grow and sustain a breakdown. All those emitted and accelerated electrons, ionized atoms require power to produce and support.
2. The surface modification created by the breakdown could very well be related to the power available. More power – rougher surface after breakdown – breakdown at lower surface electric field. All structures we see go through a conditioning process so the breakdown rate is influenced by the history.

Now comes a very messy, non-idealized, exercise in phenomenology…

We ignore standing wave cavities for the time being.

We'll decide which dimension to scale the power through intuition, guess work and by looking how the data fit.

After some tries, P divided by inner-iris circumference – the smallest constriction in the structure works pretty well.

But our data shows that frequency scaling geometries gives approximately fixed gradient, so we throw in the frequency to give:

$$Pf \;/\, C \propto const$$

$$Pf\ / C \propto const$$

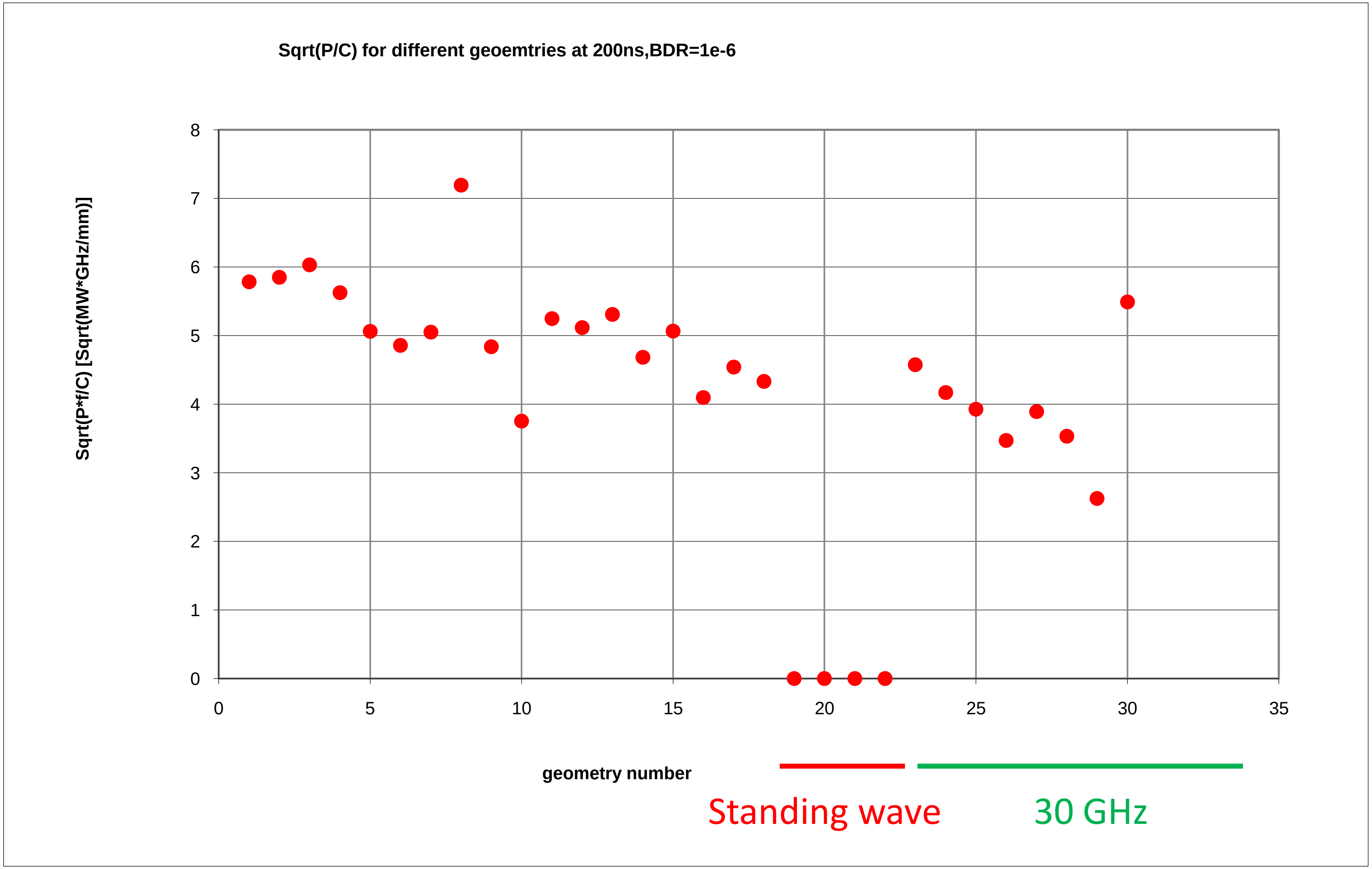

Pf/C is certainly not the whole truth. Standing wave cavities are not described correctly and the frequency (in)dependence had to be put in by hand. Plus the rule is just phenomenological.

Still *Pf/C* is sufficiently compelling that it has become one of the design criteria for CLIC main linac structures- accelerating and PETS.

But can we get closer, and *derive*, the real dependence?

Remember, the data were taken with structures with somewhat different preparation techniques and testing conditions. Plus at some level there will be residual structure-to-structure variation in performance so fitting to existing data has its limits.

So our approach has to come from the theoretical side. We will try to apply some of the ideas from section II more closely now.

Basic concepts behind a better high-gradient limit

1. Make it a local quantity that way frequency independence of fixed geometry is automatic.
2. Generalize to complex power flow to include standing wave cavities.
3. Base the power flow based limit on physics of breakdown – specifically on the ability of rf fields to feed field emission.

Qualitative picture

- Field emission currents J_{FN} heat a (potential) breakdown site up to a temperature rise ΔT on each pulse.
- After a number of pulses the site got modified so that J_{FN} increases so that ΔT increases above a certain threshold.
- Breakdown takes place.

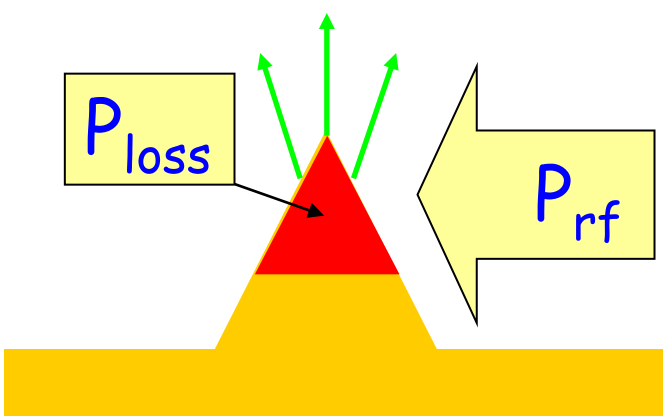

This scenario can explain:

- Dependence of the breakdown rate on the gradient (Fatigue)
- Pulse length dependence of the gradient (1D÷3D heat flow from a point-like source)

EM fields around a tip of β=30

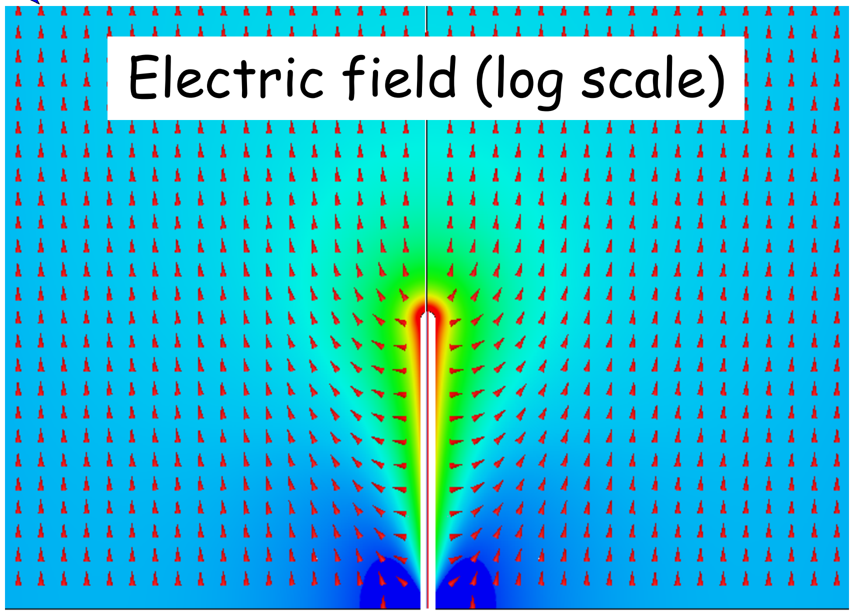

Unperturbed rf power flow:

$S = E \times H_{RF}$

$H = const$

Field emission power flow:

$S_{FN} = E \times H_{FN}$

$H_{FN} = I_{FN}/2\pi r$

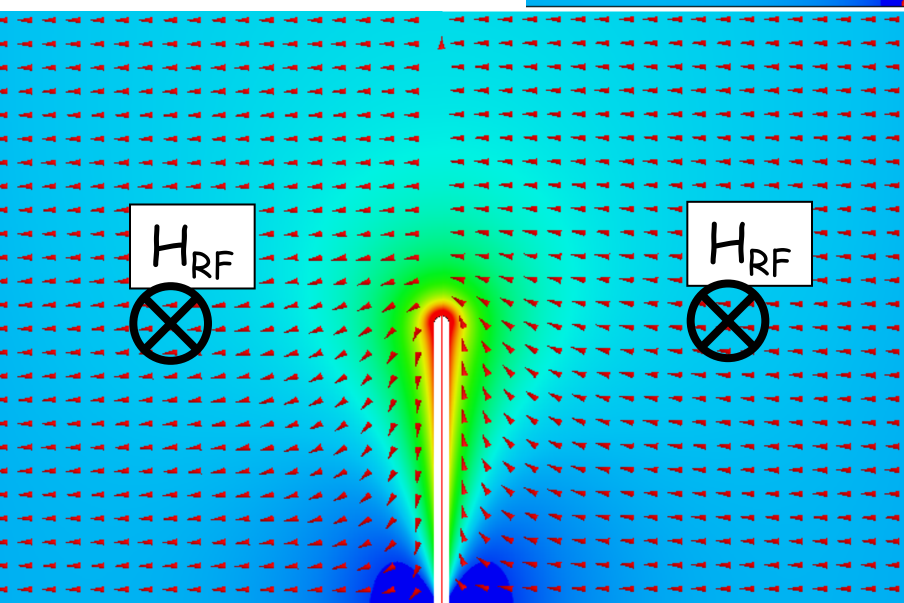

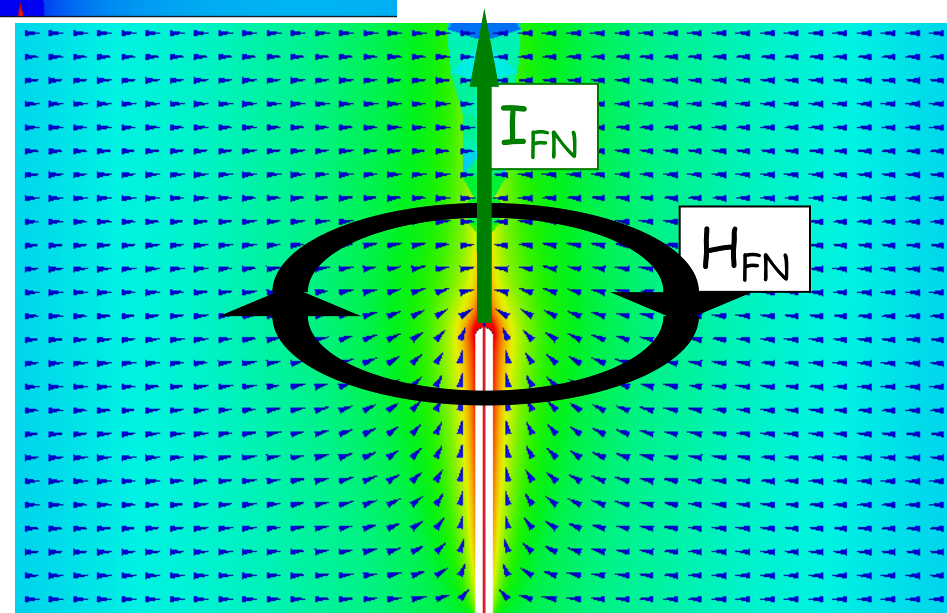

Field emission and rf power flow

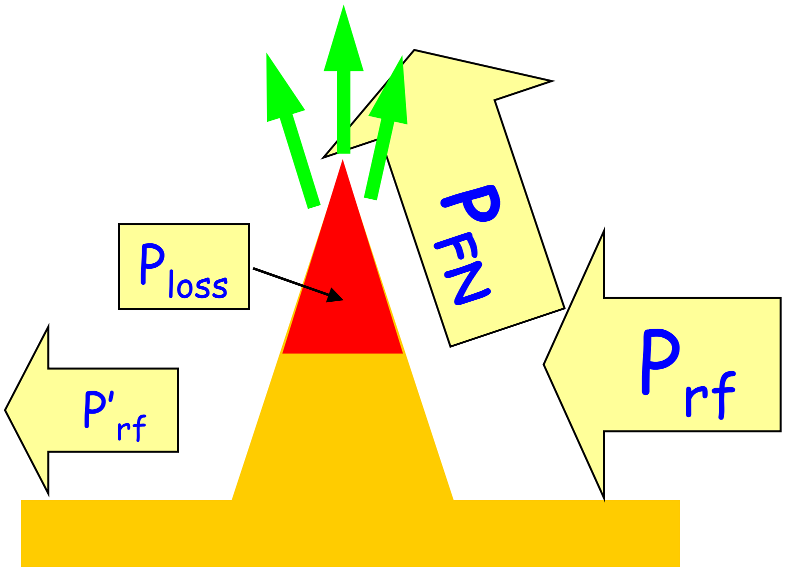

$$\Delta T \sim P_{loss} << P_{FN} \le P_{rf}$$

$$P_{loss} = \int_V J_{FN}^2 \rho \, dv$$

$$P_{FN} = \oint_S E \times H_{FN} \, ds \sim E \cdot I_{FN}$$

$$P_{rf} = \oint_S E \times H \, ds$$

There are two regimes depending on the level of rf power flow

1. If the rf power flow dominates, the electric field remains unperturbed by the field emission currents and heating is limited by the rf power flow (We are in this regime)
2. If power flow associated with field emission current P_{FN} dominates, the electric field is reduced due to “beam loading” thus limiting field emission and heating

Field emission and power flow

$$E \times H = E_0 \cdot H_0^{TW} \sin^2 \omega t + E_0 \cdot H_0^{SW} \sin \omega t \cos \omega t$$

$$I_{FN} \cdot E = AE_0^3 \sin^3 \omega t \cdot \exp\left(\frac{-62\ GV/m}{\beta E_0 \sin \omega t}\right)$$

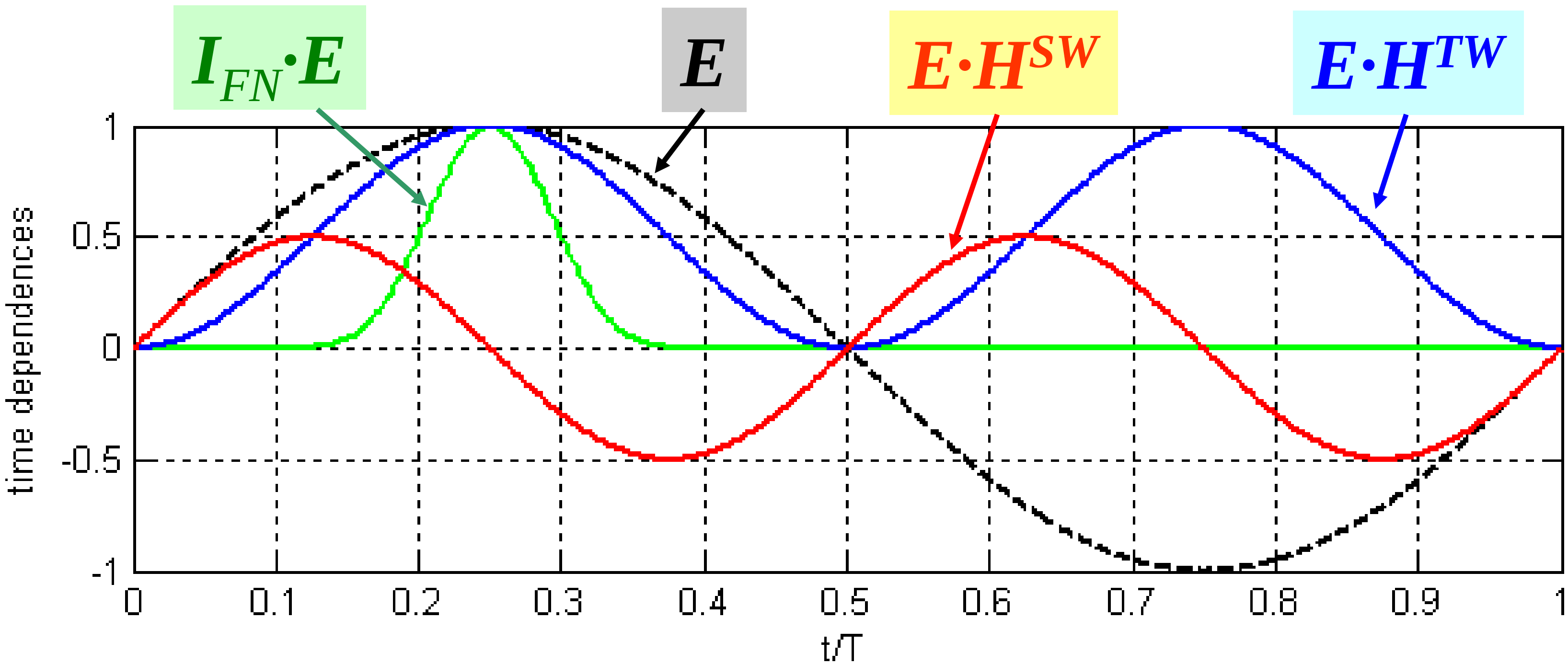

Field emission and rf power coupling

What matters for the breakdown is the amount of rf power coupled to the field emission power flow.

$$P_{coup} = \int_0^{T/4} P_{rf} \cdot P_{FN}\, dt \Bigg/ \left(\int_0^{T/4} P_{FN}\, dt \cdot \int_0^{T/4} P_{rf}\, dt \right)$$

$$= C^{TW} E_0 H_0^{TW} + C^{SW} E_0 H_0^{SW}$$

Assuming that all breakdown sites have the same geometrical parameters the breakdown limit can be expressed in terms of modified Poynting vector S_c.

$$S_c = E_0 H_0^{TW} + \frac{C^{SW}}{C^{TW}} E_0 H_0^{SW} = \mathrm{Re}\{\mathbf{S}\} + g_c \cdot \mathrm{Im}\{\mathbf{S}\}$$

Field emission and rf power coupling

Constant g_c depends only on the value of the local surface electric field βE_0

$$g_c = \frac{\int_0^{\pi/2} \sin^4 x \cos x \cdot \exp\left(\frac{-62\ GV/m}{\beta E_0 \sin x}\right) dx}{\int_0^{\pi/2} \sin^5 x \cdot \exp\left(\frac{-62\ GV/m}{\beta E_0 \sin x}\right) dx}$$

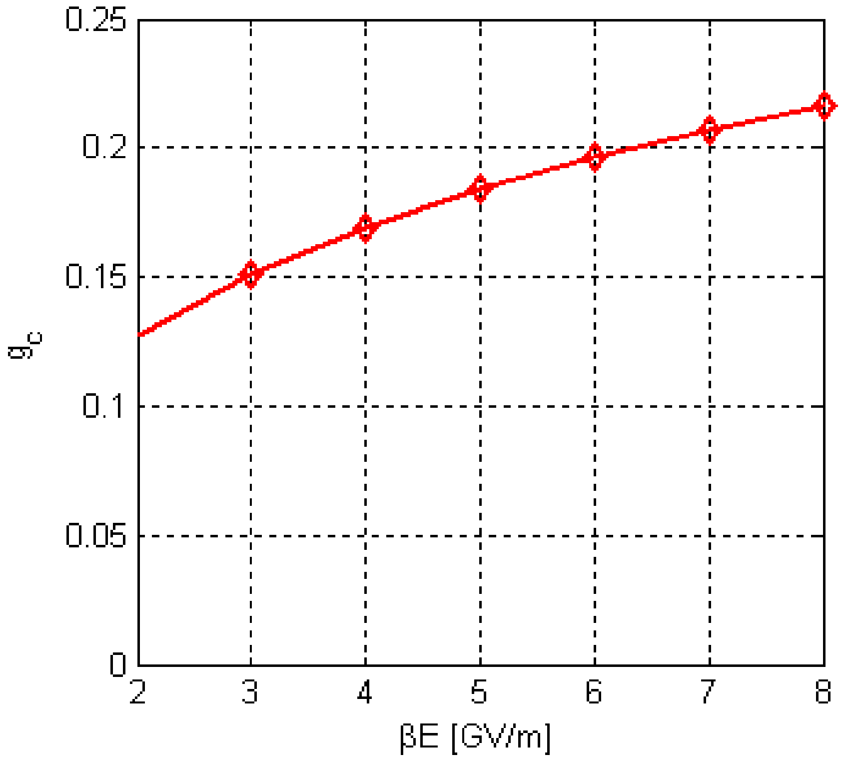

g_c is in the range: from 0.15 to 0.2

Analytical estimates for a cylindrical tip

For a cylindrical protrusion heat conduction is described by:

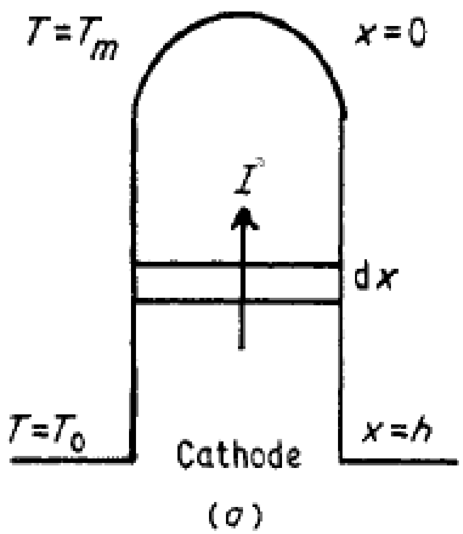

$$C_V \frac{\partial T}{\partial t} = K \frac{\partial^2 T}{\partial x^2} + J^2 \rho$$

Williams & Williams, J. Appl. Rhys. D, 5 (1972) 280

Let's get approximate solution it in two steps:

1. Solve it in steady-state (i.e. left hand side is zero) for a threshold current density required to reach melting temperature T_m
2. Solve time dependent equation in linear approximation to get the threshold time required to reach melting temperature

Analytical estimates for a cylindrical tip

Case B: Resistivity is temperature-dependent: $\rho = \rho_0 \cdot T / T_0$ (Bloch-Grüneisen)

Step 1:

$$K \frac{\partial^2 T}{\partial x^2} + J^2 \rho = 0; \quad T\Big|_{x=h} = T_0; \; T\Big|_{x=0} = T_m; \; \frac{\partial T}{\partial x}\Big|_{x=0} = 0$$

$$T = T_m \cos \sqrt{\frac{J^2 \rho_0}{K T_0}} x; \quad J_m^{\rho 1} = \sqrt{\frac{K T_0}{h^2 \rho_0}} \arccos \frac{T_0}{T_m}$$

Step 2:

$$C_V \frac{\partial T}{\partial t} = J^2 \rho; \quad T\Big|_{t=0} = T_0; \quad T\Big|_{t=t_m} = T_m$$

$$T = T_0 \exp \frac{J^2 \rho_0}{C_V T_0} t; \quad \tau_m^{\rho 1} = \frac{C_V T_0}{J^2 \rho_0} \ln \frac{T_m}{T_0} = \frac{C_V}{K} h^2 \ln \frac{T_m}{T_0} \Big/ \arccos^2 \frac{T_0}{T_m}$$

Analytical estimates for a cylindrical tip

Fundamental constants for copper	
Thermal conductivity: K [W/m·K]	400
Volumetric heat capacity: C_V [MJ/m^3·K]	3.45
Resistivity@300K: ρ_0 [nΩ·m]	17
Melting temperature: T_m [K]	1358

Some numbers for Case B: $\rho = \rho_0 \cdot T/T_0$

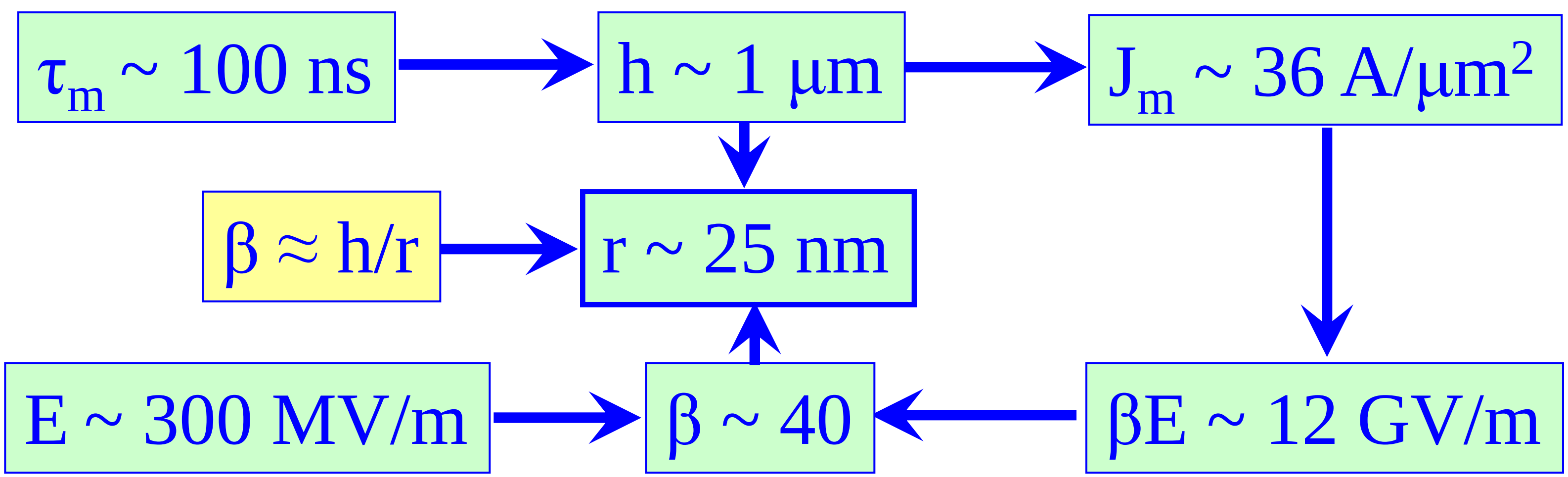

Analytical estimates for a cylindrical tip

Some numbers for Case 2: $\rho = \rho_0 \cdot T/T_0$ (Continue)

$\beta \sim 40$

$E \sim 300$ MV/m

$J_m \sim 36$ A/μm^2

$S_{FN} \sim 3.4$ W/μm^2

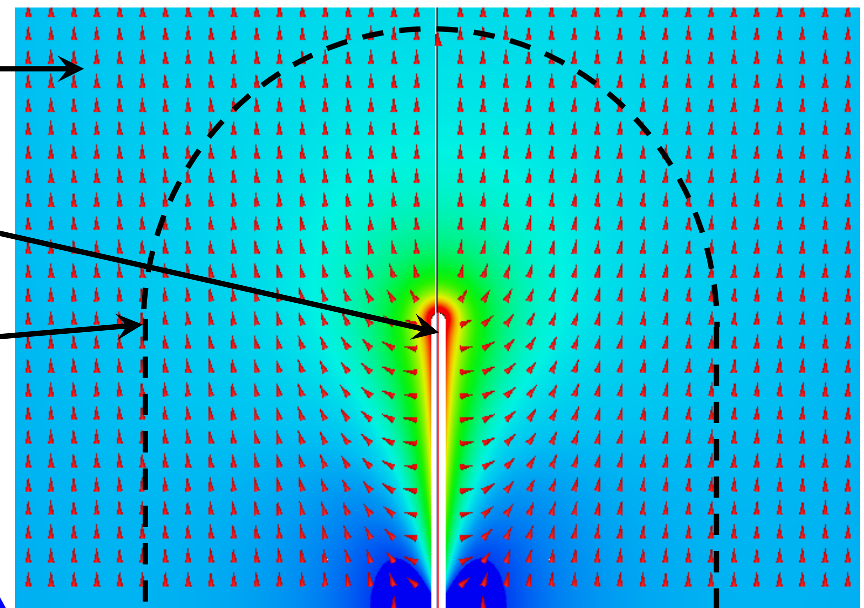

$r \sim 25$ nm

$h \sim 1$ μm

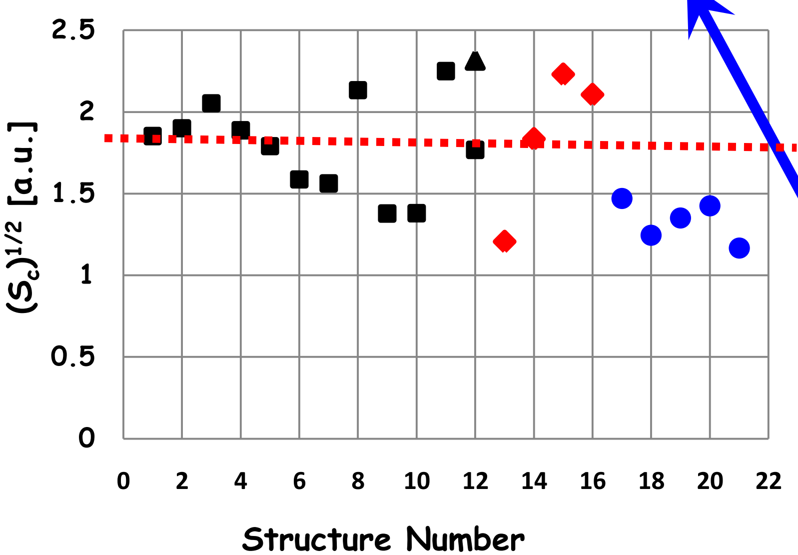

$$S_{FN}\big|_h = E\,H_{FN} = E\,\frac{J\pi r^2}{2\pi h} = E\,\frac{J r}{2\beta}$$

S_c

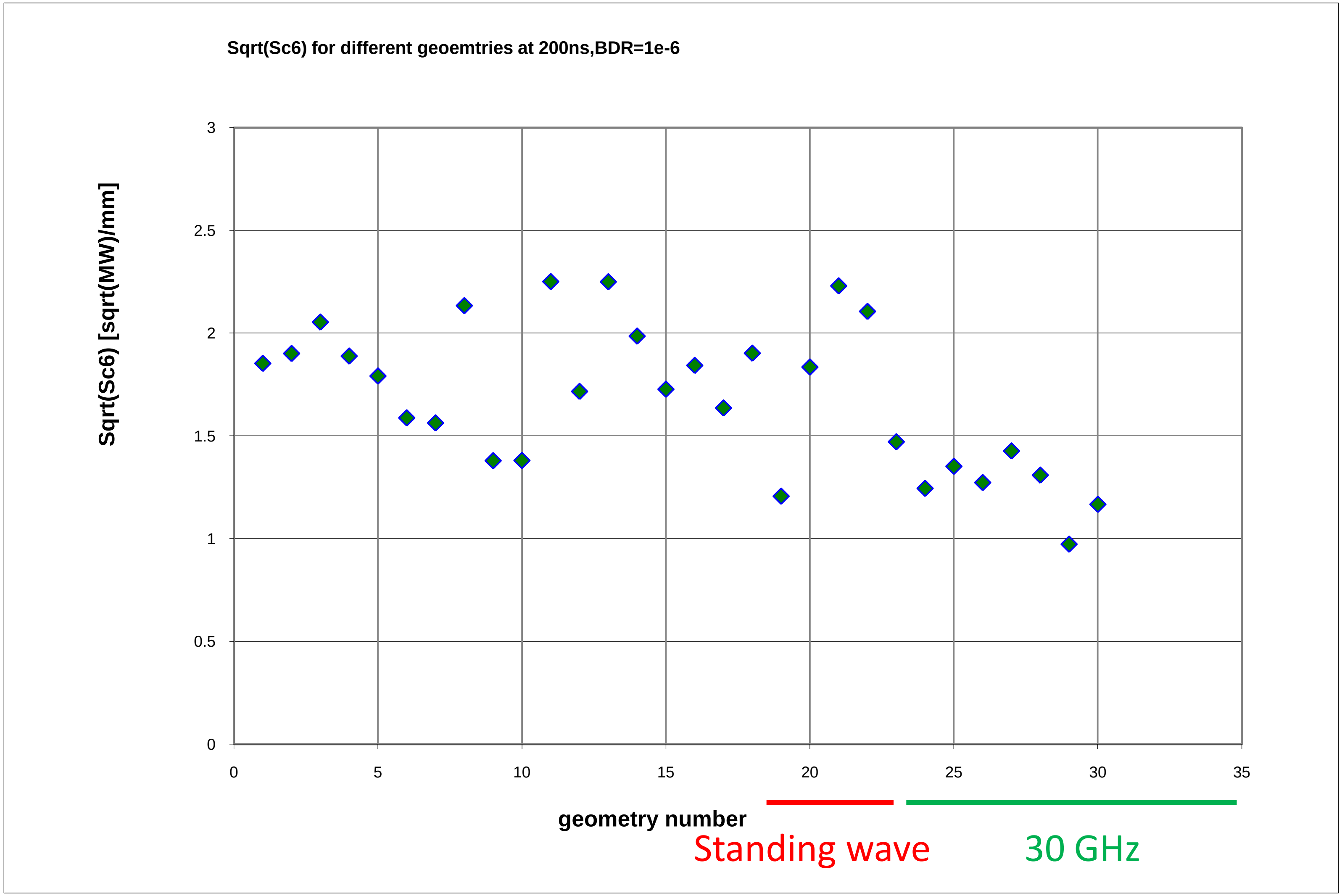
Sqrt(Sc6) for different geoemtries at 200ns,BDR=1e-6
Sqrt(Sc6) [sqrt(MW)/mm]
3
2.5
2
1.5
1
0.5
0
0
5
10
15
20
25
30
35
geometry number
Standing wave
30 GHz

Sc and P/C as criteria

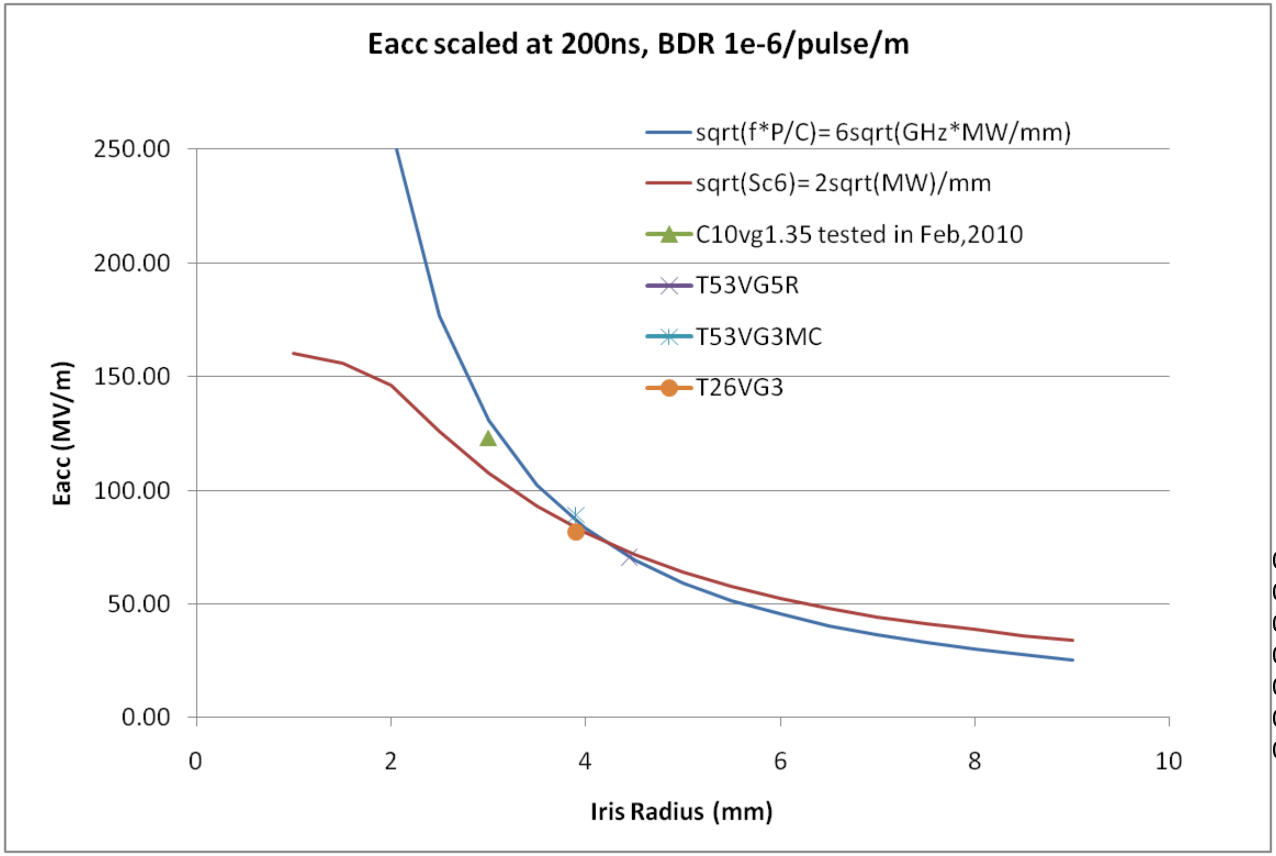

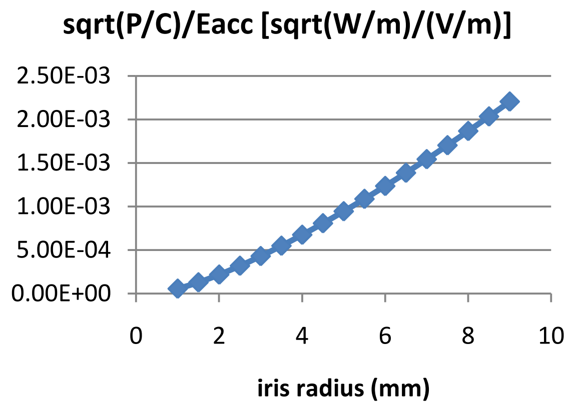

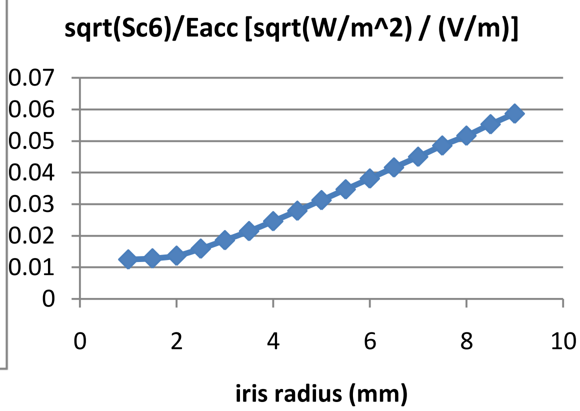

P: the power flow, C: the circumference of the iris

Sc6: modified poynting vector ***Real(Poynting)+Imag(Poynting)/6*** [1]

The value **sqrt(f*P/C)=6 sqrt(GHz*MW/mm)** and **sqrt(Sc6)=2 sqrt(MW)/mm** are based on some high power test results [1]

[1] A. Grudiev, S. Calatroni, and W. Wuensch Phys. Rev. ST Accel. Beams 12, 102001 (2009)

To conclude:

I would now like to review a few selected slides from my plenary talk during ILWS2010, emphasizing the connections with these lectures.

Accelerating structures – specifications

High-gradient:

1. 100 MV/m loaded gradient
2. 170 (flat top)/240 (full) ns pulse length
3. $<4\times10^{-7}$ 1/pulse/m breakdown rate

Beam dynamics:

1. 5.8 mm diameter minimum average aperture (short range transverse wake)
2. < 1 V/pC/mm/m long-range transverse wakefield at second bunch (approximately x100 suppression).

Accelerating structures – features

E_s/E_a H_s/E_a S_c/E_a^2

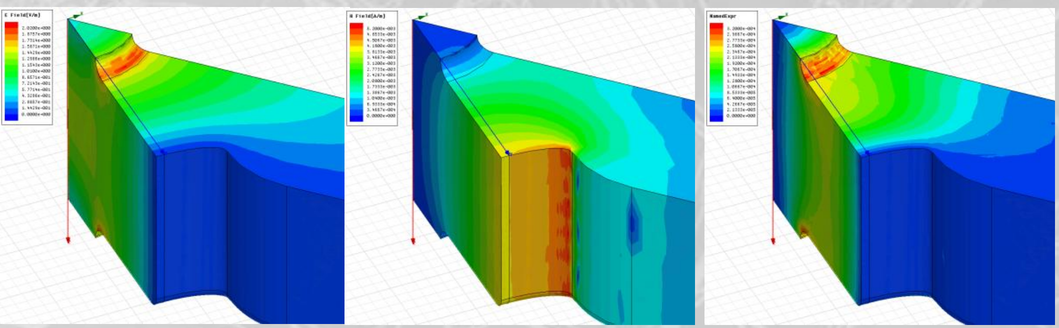

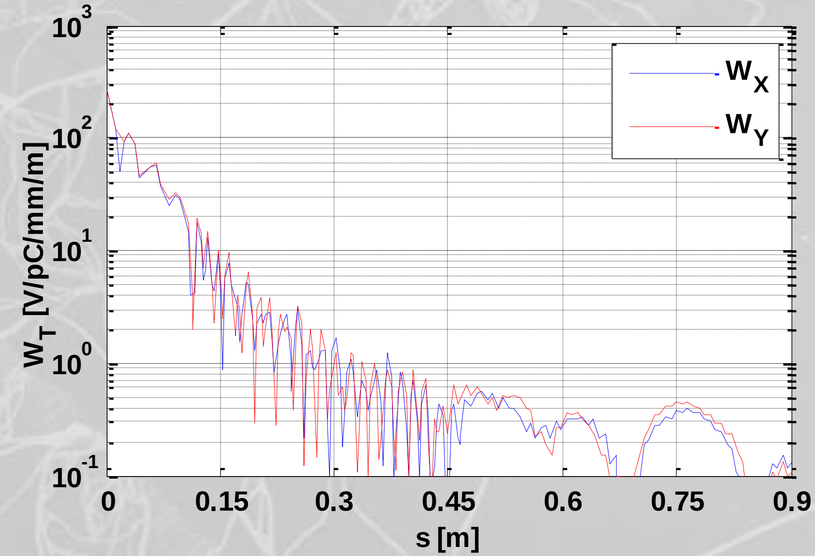

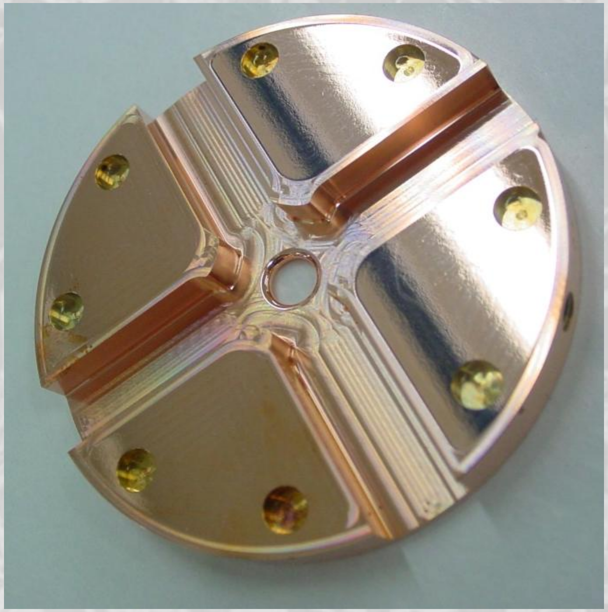

$S_c^{½}$ [MW/mm²]
E_s max [MV/m]
E_{acc} [MV/m]
ΔT [°C]
dashed – unloaded
solid – loaded

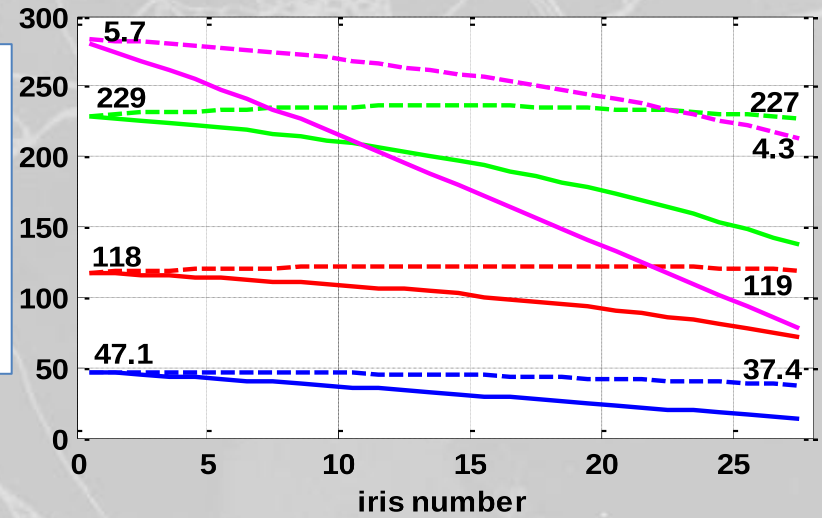

Accelerating structures – manufacture

Diffusion Bonding of T18_vg2.4_DISC

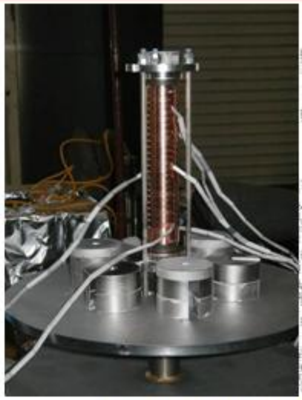

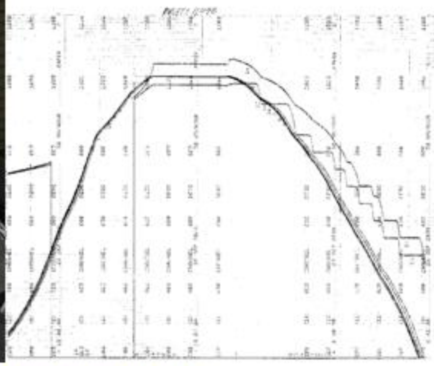

Pressure: 60 PSI (60 LB for this structure disks)
Holding for 1 hour at 1020° C

Vacuum Baking of T18_vg2.4_DISC

650° C
10 days

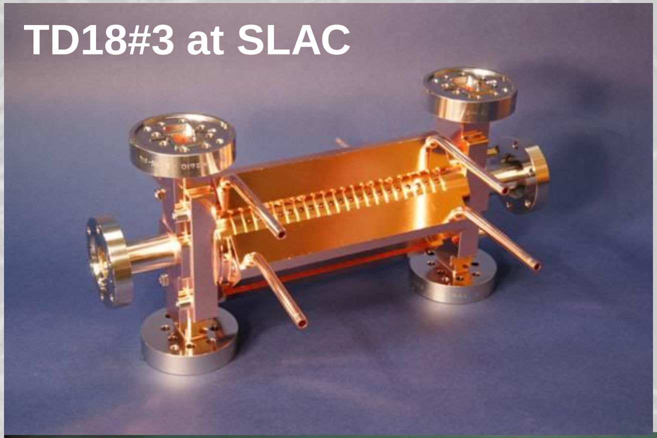

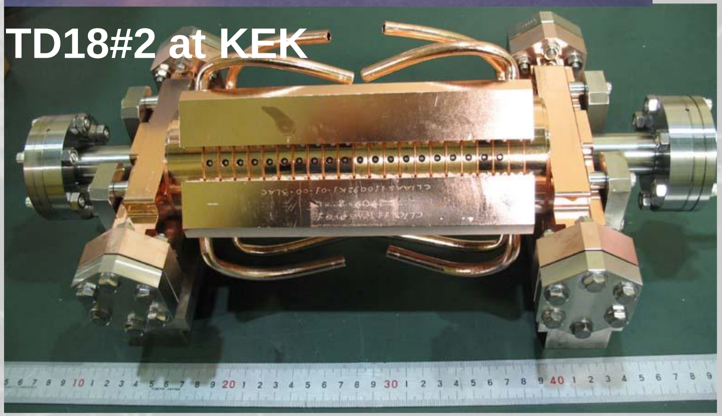

Preparation for high-gradients

Our baseline treatment for high-gradient was developed by the NLC/JLC program.

Our current understanding of *why exactly* it works comes from our ongoing breakdown physics study. Crystal dislocations appear to be the cause of our gradient limit (ok, there is still a debate!).

1. **Etching** –Etching occurs preferentially at dislocations due to lower local work function. This is particularly important for milled surfaces, which have significant induced stress and consequently high dislocation density. Also removes particles.
2. **1050 °C hydrogen fire**– Near melting point results in significant annealing. Relieves stresses and reduces dislocation density. Excellent removal of chemical contaminants.

Summary of CLIC accelerating structure test results

Structure type	Fabrication	Test location	Total testing time [hr]	Unloaded gradient [MV/m]	Flat top pulse length [ns]	Breakdown rate [1/pulse/meter]
T18	KEK/SLAC	SLAC	1400	105	230	1.6×10^{-6}
T18	KEK/SLAC	KEK	3900	102	252	8×10^{-7}
T18	KEK/SLAC	SLAC	280	110	230	7.7×10^{-5}
T18	CERN	SLAC	550	90	230	1.3×10^{-6}
TD18	KEK/SLAC	SLAC	1300	85 (a)	230	2.4×10^{-6}
				100 (b)	230	7.6×10^{-5}
TD18	KEK/SLAC	KEK	3200	87 (a)	252	2×10^{-6}
				102 (b)	252	1.4×10^{-5}
T24	KEK/SLAC	SLAC	200	92	200	9.8×10^{-5}
TD24	CERN	TBTS	<1 (0.8Hz)	55	≈ 100	$O(10^{-2})$

conditioning continues (a) BDR specification run (b) gradient specification run

Synthesis of accelerating structure test results scaled to CLIC breakdown rate

Scaling to CLIC conditions: Scaled from lowest measured BDR to BDR=4*10^{-7} and τ=180 ns (CLIC flat-top is 170 ns), using standard $E^{29}\tau^5/BDR$=const. Correction to compensate for beam loading not included – expected to be less than about 7%.

Breakdown rate evolution with extended running

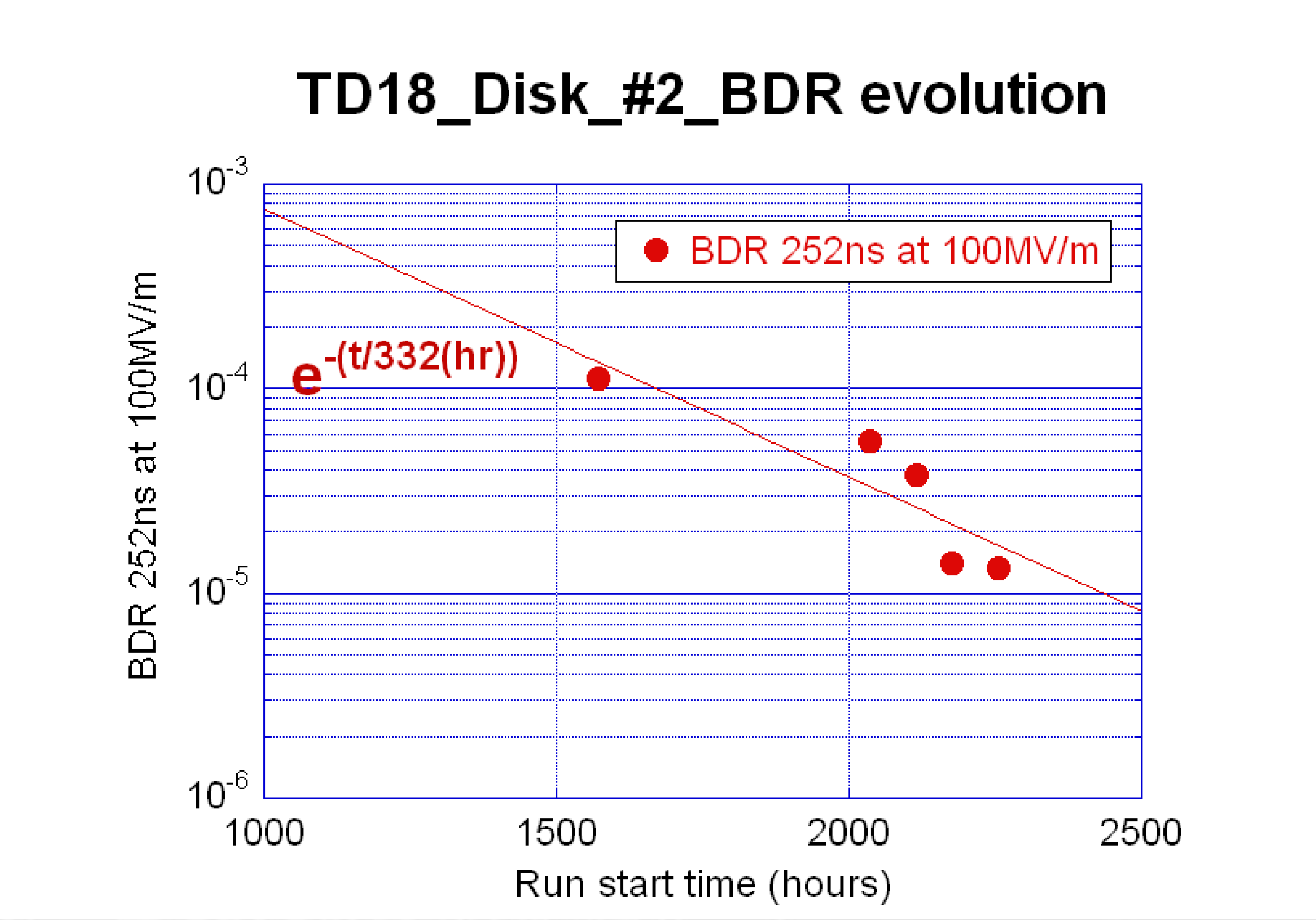

TD18 test at KEK